Genes & Diseases (2021) 8, 849–866

Available online at www.sciencedirect.com

ScienceDirect

journal homepage: http://ees.elsevier.com/gendis/default.asp

FULL LENGTH ARTICLE

Suppression of a core metabolic enzyme dihydrolipoamide dehydrogenase (*dld*) protects against amyloid beta toxicity in *C. elegans* model of Alzheimer's disease

Waqar Ahmad*, **Paul R. Ebert**

School of Biological Sciences, The University of Queensland, Brisbane, QLD 4072, Australia

Received 20 May 2020; received in revised form 24 July 2020; accepted 14 August 2020
Available online 20 August 2020

KEYWORDS
Alzheimer's disease;
Amyloid beta;
C. elegans;
Dihydrolipoamide dehydrogenase (*dld*);
Energy metabolism;
Neurodegeneration;
Proteomics

Abstract A decrease in energy metabolism is associated with Alzheimer's disease (AD), but it is not known whether the observed decrease exacerbates or protects against the disease. The importance of energy metabolism in AD is reinforced by the observation that variants of dihydrolipoamide dehydrogenase (DLD), is genetically linked to late-onset AD. To determine whether DLD is a suitable therapeutic target, we suppressed the *dld-1* gene in *Caenorhabditis elegans* that express human Aβ peptide in either muscles or neurons. Suppression of the *dld-1* gene resulted in significant restoration of vitality and function that had been degraded by Aβ pathology. This included protection of neurons and muscles cells. The observed decrease in proteotoxicity was associated with a decrease in the formation of toxic oligomers rather than a decrease in the abundance of the Aβ peptide. The mitochondrial uncoupler, carbonyl cyanide 4-(trifluoromethoxy) phenylhydrazone (FCCP), which like *dld-1* gene expression inhibits ATP synthesis, had no significant effect on Aβ toxicity. Proteomics data analysis revealed that beneficial effects after *dld-1* suppression could be due to change in energy metabolism and activation of the pathways associated with proteasomal degradation, improved cell signaling and longevity. Thus, some features unique to *dld-1* gene suppression are responsible for the therapeutic benefit. By direct genetic intervention, we have shown that acute inhibition of *dld-1* gene function may be therapeutically beneficial. This result supports the hypothesis that lowering energy metabolism protects against Aβ pathogenicity and that DLD warrants further investigation as a therapeutic target.

* Corresponding author.
E-mail addresses: waqar.ahmad@uqconnect.edu.au (W. Ahmad), p.ebert@uq.edu.au (P.R. Ebert).
Peer review under responsibility of Chongqing Medical University.

https://doi.org/10.1016/j.gendis.2020.08.004

Introduction

One of the main pathological hallmarks of AD that underlies the neuronal dysfunction and dementia is extracellular accumulation of amyloid beta (Aβ) plaques resulting from protein misfolding.[1] In addition to the accumulation of Aβ, neuroimaging studies of AD brains found impaired glucose metabolism and diminished activities of mitochondrial enzymes at latter stages of the disease.[2–5] The cause and effect relationships between these observations are unclear as impairment of energy metabolism may induce protein misfolding, leading to formation of Aβ plaques, but the opposite may also be true as production and accumulation of Aβ may also damage energy metabolism.[6–14]

The difficulty in understanding the role of metabolic decline on AD relates to the inaccessibility of AD affected brains during progression of the disease. This situation makes it difficult to distinguish cause from consequence and necessitates reliance on AD disease models. The decrease in energy metabolism in AD has been interpreted in two opposing ways; as a main cause of AD, or as a protective response against the symptoms of the disease. The first interpretation is mostly supported by studies conducted at a late stage of the disease on post-mortem brains, making it difficult to assign causality.[15–19] In contrast, several studies on mixed stage AD samples support that the down-regulation of energy metabolism is a protective factor, leading to the hypothesis that a decrease in nutrient and oxygen supply minimizes neural activity, thereby decreasing the repair burden.[20,21] This is supported by results from a transgenic mouse model of AD in which upregulation of aerobic respiration is clearly harmful.[22]

Increased risk of late-onset AD is genetically linked to the human *dld* locus.[23] Furthermore, inhibition of DLD enzyme activity using 5-methoxyindole-2-carboxylic acid (MICA) protects against the toxicity of human Aβ in transgenic *Caenorhabditis elegans*.[24] Moreover, *dld-1* suppression also improved the acetylcholine neurotransmission in human tau model of Alzheimer's disease.[25] The DLD enzyme is a subunit of three ketoacid dehydrogenase complexes, each of which contributes to energy metabolism, pyruvate dehydrogenase complex PDH, α-ketoglutarate dehydrogenase complex (KGDH) and branched chain ketoacid dehydrogenase complex (BCKDH).[26,27] Reduced levels of these enzymes in post-mortem brain tissues and fibroblasts of patients with either Alzheimer's or Parkinson's disease indicate a direct link between energy metabolism and AD.[28–33] As targeted disruption of DLD can also reduce the activities of KGDH and PDH,[34] thus, a direct link between DLD activity and AD progression is a distinct possibility.

To explore the relationship between metabolism and AD, we suppressed *dld-1* in the nematode *C. elegans* that expresses human Aβ. *C. elegans* is well-suited for such studies as it has been used extensively to study the metabolic profiling and overlapping, genetics of aging and associated age-related diseases such as AD.[35–37] A decrease in Aβ mediated pathology in response to suppression of *dld-1* supports the notion that decreased energy metabolism is neuroprotective.

Materials and methods

Nematode strains

Caenorhabditis elegans strains used in this study are the wild type strain, N2 (Bristol), and the long-lived, stress resistant *dld-1* mutant, *dld-1*(*wr4*). *dld-1*(*wr4*) strain contains a A460V missense mutation and showed resistance against phosphine exposure that can also be achieved using *dld-1* RNAi in wild type.[38,39] Strains expressing human β-amyloid peptide in muscle cells include CL2006 (*dvIs2* [*unc-54*::Aβ1-42) + *rol-6*(su1006)]), which produces the human Aβ peptide constitutively and CL4176 (*smg-1*(cc546) *dvIs27* [*myo*-3::Aβ1-42::3′-UTR(long)]) in which the temperature increase from 16 °C to 23 °C prevents degradation of the abnormally long transcript from the Aβ transgene by SMG-1(*cc546*), a temperature sensitive version of an essential component of the RNA surveillance system. The double mutant strain CL802 (*smg-1*(cc546);*rol-6*(su1006)) was used as a control for CL2006 and CL4176 in assaying paralysis/movement. The use of these strains as a worm model of AD was documented previously.[40] We used strain CL2355 (*smg-1*(cc546) *dvIs50*[*snb-1*::Aβ1-42::3′ UTR(long) + *mtl-2*::*gfp*]), in which Aβ is expressed pan neuronally, to complement studies on the strains in which Aβ was expressed in muscle cells. The control strain for CL2355 was CL2122 (*dvIs15*[*mtl-2*::*gfp*]).[40–43] Sod-3::GFP reporter strain CF1553 (*muIs84* [*sod-3p*::*GFP* + *rol-6*(su1006)]) was also used in this study.

Culture conditions

Mixed-stage cultures of *C. elegans* were maintained on nematode growth medium (NGM) seeded with *E. coli* OP50 at 20 °C, except strains CL4176 and CL2355, which were maintained at 16 °C to suppress Aβ expression. Synchronised cultures for bioassays were obtained by standardized protocols described previously.[40–43] Wild type, *dld-1*(*wr4*) mutant and Aβ transgenic worms CL4176 were all initially cultured at 16 °C for 36 h after which the temperature was increased to 23 °C for 36 h except for the paralysis assay for which the temperature was further increased to 25 °C to maximise expression of the Aβ transgene. Phenotypes of the worms were monitored by visual observation under a microscope and/or quantified using the WormScan procedure.[44]

dld-1 gene suppression by RNAi

Control empty vector L4440 and RNAi clone sjj-LLC1.3 were developed in the same bacterial strain known as HT115. The *E. coli* strain HT115, which expresses double-stranded RNA of the *dld-1* gene (sjj-LLC1.3) was fed to each of the four *C. elegans* strains to suppress expression of the *dld-1* gene.[45] Briefly, the bacteria were cultured in LB medium containing 100 μg/mL ampicillin overnight with shaking at 37 °C. 300 μL of this bacterial culture was transferred to NGM plates containing 100 μg/mL ampicillin and 1 mM IPTG. The plates were incubated at 25 °C overnight to allow the bacteria to grow. Synchronised L1 worms were transferred to the bacterial plates and kept at 16 °C for 36 h. After a

further 36 h at 25 °C the worms were ready for use in the assays described below. Mock gene suppression controls were treated in exactly the same way except that the bacterial strain (HT115) for the controls contained the plasmid vector without the *dld-1* gene fragment.

Paralysis and mortality assays

Paralysis can be defined as a time-dependent observable decrease in muscle activity, which may lead to complete cessation of movement. Paralysis can be inhibited or reversed.[46] Mortality in this study refers to acute death caused by decline of cellular functions and organelles. In practice, these can be difficult to distinguish, so we relied on the published descriptions of the assays that we used to determine whether the results should be referred to as mortality or paralysis. Synchronised, L1 stage worms were transferred to NGM plates that had been seeded with either the *dld-1* RNAi or empty vector strain of *E. coli*, the latter of which contains an empty vector as an RNAi control. After 36 h at 16 °C, worms were upshifted to 25 °C. The worms were then scored for paralysis every second hour after an initial 24-h period until the last worm became paralysed. For mortality assays, worms were counted as dead or alive after treatment.

Touch response assay

Touch response assays were performed at 20 °C on synchronised L4 worms after inducing Aβ expression for 36 h at 23 °C. Fifteen animals of each strain were selected arbitrarily and put on freshly made NGM plate. Worms were left on plates for 2 min to allow them to equilibrate to the new conditions. Worms were then touched on the head or tail region using a platinum wire to stimulate locomotion and body bends were then counted for 30 s.

Aldicarb and levamisole assays

Worms prepared as described for *dld-1* gene suppression were incubated in the presence of 1 mM aldicarb, an acetylcholinesterase inhibitor.[47] In parallel with the aldicarb experiment, we also exposed worms to 0.2 mM levamisole, a cholinergic receptor agonist.[48] The number of active worms was counted every hour until all worms became paralyzed.

Phosphine exposure assay

Nematodes were fumigated with phosphine at 500 ppm and 2000 ppm as described previously.[49] Briefly, a synchronised population of 48 h old (L4) nematodes was washed with M9 buffer and approximately 80—100 nematodes were transferred to each well of 12-well tissue culture plates containing 2.5 mL of NGM agar per well pre-seeded with *E. coli*; either the empty vector or the RNAi. Nematodes were exposed to phosphine for 24 h in glass fumigation chambers, after which the chambers were opened and the worms were allowed to recover for 48 h in fresh air. The numbers of surviving nematodes were then counted.

5-HT sensitivity assay

To determine the level of Aβ-induced 5-HT hypersensitivity, serotonin (creatinine sulfate salt) was first dissolved in M9 buffer to 1 mM as described previously.[43] Synchronized worms were then washed with M9 buffer and transferred into 200 μl of the 1 mM serotonin solution in 12-well assay plates. The worms were scored as either active or paralysed after 5 min.

Chemotaxis assays

Chemotaxis assays was performed as described previously[50] with minor changes. Briefly, L1 worms of Aβ-expressing strain CL2355 and their no-Aβ control strain CL2122 were incubated at 16 °C for 36 h on NGM plates containing 100 μg/mL ampicillin, and 1 mM IPTG seeded with either an empty vector or *dld-1* RNAi strain of *E. coli*. The temperature was then up-shifted to 25 °C for a further 36 h. L4 stage worms were collected and washed with M9 buffer. After washing, worms were placed on the centre of the assay plate (with or without *dld-1* RNAi expressing *E. coli* lawn). Attractant (0.1% benzaldehyde in 100% ethanol) as a containing 1 μl spot, was added to one edge of the plate with 1 μl of 100% ethanol as a control on the opposite side of the plate. 1 μl of 1M sodium azide was added to each of the two spots to immobilize the animals once they had migrated to one or the other destination. The chemotaxis index (CI) (number of worms at the attractant location number of worms at the control location]/total number of worms on the plate) was calculated after 2 h of incubation at 23 °C.

Egg hatching assay

Wild type (N2), no Aβ control (CL2122) and the Aβ transgenic strain (CL2355) were synchronised and grown to maturity at 16 °C (L4 stage, 4 days of age). 10 individuals were then transferred to fresh agar plates and the temperature was shifted to 23 °C. After 24 h of incubation, adult worms were removed from the plates. Unhatched eggs and larvae were counted every 24 h for the next three days.

Uncoupler treatment

L4 worms were exposed to 17.5 μM of the mitochondrial uncoupler carbonyl cyanide 4-(trifluoromethoxy)phenylhydrazone (FCCP). This dose does not cause significant mortality of wild type nematodes.[51] Mortality was scored immediately after a 24-h exposure to FCCP at 23 °C.

Oxidative stress measurement

sod-3 expression

The response to mitochondrial superoxide-mediated oxidative stress was measured using *sod-3*::GFP in strain CF1553. Synchronized worms were fed with *E. coli* containing either empty vector or vector that expresses double stranded RNA corresponding to the *dld-1* gene for 72 h at 20 °C. Quantification of *sod-3* levels was carried out using a

fluorescence microscope (excitation filter: 485 nm, emission filter: 530 nm) by subtracting, non-worm background fluorescence from fluorescence of the worms themselves.

RO/NS measurement

Reactive oxygen/nitrogen species (RO/NS) levels were measured using 2′,7′-dichlorofluorescein diacetate (DCF-DA) as described previously with modifications.[52] Briefly, worms were synchronized and placed on NGM plates seeded with *E. coli* containing either empty vector or vector that expresses double stranded RNA corresponding to the *dld-1* gene. After 36 h at 16 °C followed by a temperature upshift for a further 36 h at 23 °C, worms were washed with PBS three times and snap frozen in 250 μl cell lysis solution (20 mM Tris pH 7.5 50 mM EDTA 200 mM NaCl 0.5% SDS). To prepare extracts, worms were sonicated followed by centrifugation at 14,000 rpm for 30 min in a refrigerated microcentrifuge. The supernatant was collected and further used for protein quantification using a nanodrop spectrophotometer. Supernatant containing 25 μg of protein was pre-incubated with 250 μM DCF-DA in 100 μl of 1× PBS at 37 °C for 1 h. Fluorescence intensity (excitation wavelength 485 nm and emission wavelength 535 nm) was measured using SpectraMax M3 fluorometer (Molecular Devices, Sunnyvale, USA). The fluorescence intensity was corrected by subtracting background fluorescence of 250 μM DCF-DA from each sample.

H_2O_2 spectrophotometric measurement

Hydrogen peroxide (H_2O_2) levels were measured spectrophotometrically using toluidine blue as described previously by Sunil et al with minor modifications.[53] Worms extracts were prepared and quantified as described above in the DCF-DA assay protocol. For each 25 μg of protein we added 20 μl 2% potassium iodide, 20 μl 2 M HCl, 10 μl 0.01% toluidine blue and 40 μl 2 M sodium acetate. The contents were mixed and absorbance was measured at 628 nm H_2O_2 concentration was calculated using an H_2O_2 concentration curve.

Quantitative RT-PCR

Synchronised L1 stage *C. elegans* of the wild type strain N2 or the Aβ-expressing strain CL4176 were fed *E. coli* containing empty vector or a *dld-1* RNAi plasmid. After 36 h at 16 °C, the temperature was raised to 23 °C for 48 h and worms were collected for RNA extraction. Total RNA was extracted using the acid-phenol (Trizol) method and converted to single stranded cDNA using an Invitrogen SuperScript cDNA synthesis kit following the prescribed protocol. Gene specific primers were designed using NCBI Primer-BLAST as follows: Aβ forward primer CCGACATGACTCAGGATATGAAGT, Aβ reverse primer CACCATGAGTCCAATGATTGCA; *dld-1* forward primer GATGCCGATCTCGTCGTTAT, *dld-1* reverse primer TGTGCAGTCGATTCCTCTTG; *act-1* forward primer CGCTCTTGCCCCATCGTAAG, *act-1* reverse primer CTGTTGGAAGGTGGAGAGGG; *gpd-2* forward primer TTCTCGTGGTTGACTCCGAC, and *gpd-2* reverse primer AGGGAGGAGCCAAGAAGGTAAC. Aβ or *dld-1* mRNA levels in worms were quantified using Rotor Gene Q (QIAGEN) thermocycler. The PCR conditions were 95 °C for 30 s followed 35 cycles of 95 °C for 20 s, 55 °C for 30 s, and 72 °C for 40 s. For qPCR, SYBR® Green JumpStart™ ReadyMix™ (Sigma) was used. The relative gene expressions were monitored using the *gpd-2* or *act-1* genes by the $2^{\Delta\Delta Ct}$ method.

Western blotting of DLD and Aβ

*A*β was identified in *C. elegans* strains by immunoblotting after separation on a 16% Tris-Tricine gel. A standard Western blotting protocol was used except that SDS was omitted from the transfer buffer. Briefly, synchronized L4 worms were incubated at 23 °C for 48 h and were then washed with distilled water and quickly frozen in liquid nitrogen. Flash frozen worms were either stored at −80 °C or sonicated twice in ice cold cell lysis buffer (50 mM HEPES, pH 7.5, 6 mM $MgCl_2$, 1 mM EDTA, 75 mM sucrose, 25 mM benzamide, 1 mM DTT and 1% Triton X-100 with proteinase inhibitor cocktail (P2714, Sigma) and phosphatase inhibitor cocktail 3 (P0044, Sigma) according to manufacturer protocol. After sonication, the lysate was centrifuged at 10,000 rpm to remove insoluble debris and total protein in the supernatant was measured using a Pierce Coomassie (Bradford) protein assay kit (Thermo Scientific) on a NanoDdrop spectrophotometer. From each sample, 80—100 μg of total protein was precipitated with acetone and dissolved in Novex® Tricine SDS sample buffer (LC1676, Invitrogen) by heating to 99 °C for 5 min. Samples were subjected to gel electrophoresis at 100 V for 2.5 h in separate cathode (100 mM Tris, 100 mM Tricine, 0.1% SDS, pH 8.3) and anode (0.2 M Tris, pH 8.8) running buffers. Proteins were transferred onto nitrocellulose membranes by electroblotting in transfer buffer (35 mM glycine, 48 mM Tris (pH 8.8) and 20% methanol) for 70 min at 100 V and stained with Ponceau S (0.1% Ponceau S in 1% acetic acid) for 5 min following de-staining with 10% acetic acid (5 min) and washing under water 3 times or until smell of acetic acid was completely removed.

For Aβ, the membranes were blocked overnight in 5% skim milk at 4 °C to prevent non-specific binding of antibodies. The primary antibody staining was done using the Aβ monoclonal antibody 6E10 (Covance) at 1:1000 dilution in TBS (50 mM Tris, 150 mM NaCl, pH 7.6) containing 1% skim milk for 3—4 h at room temperature following three washes with TBS-T 5 min each.

For DLD detection, anti-lipoamide dehydrogenase antibody (ab133551) was used according to the same procedure except 5% BSA in 1X TBST was used. Anti-mouse IgG alkaline phosphatase antibody produced in goat (A3562, Sigma), and anti-rabbit IgG alkaline phosphatase antibody produced in goat (A3687, Sigma) were used as secondary antibody at 1:10,000 dilution in TBS containing 1% skim milk or in 1% BSA in 1X TBST. Secondary antibody staining was done for 1 h at room temperature. After washing the membrane with TBST, the proteins were detected using BCIP/NBT substrate system (Sigma) or BCIP/NBT kit (002209) from Lifetechnologies dissolved in 1M Tris (pH 9.0).

Mass spectrometry analysis

Shotgun proteomics was used to get insight the metabolic changes after *dld-1* suppression in worms expressing Aβ. A

modified protocol of Sobczyk et al and Baumann et al[54,55] was followed and worm lysate(s) collected after sonication as described in Western blotting section were used to prepare samples for protemics. Briefly, 100 μg lysate was reduced with 150 μl of 10 mM dithiothreitol (DTT) for 1 h at 60 °C followed by alkylation with 50 mM idoacetamide for 30 min in dark at 25 °C. The protein was digested with trypsin (1:50, enzyme::substrate ratio) overnight at 37 °C. After digestion, the supernatants were transferred to new 1.5 ml Protein Low-Bind tubes individually and evaporated in SpeedVac at 45 °C until fully dry. The dried samples were re-suspended in 10 μl 5% ACN/0.1% TFA and purified using ZipTip C-18 (ref) prior subjecting to mass spectrometry analysis. Reverse-phase chromatography on a Shimadzu Prominence nano LC system was use to analyse the samples. Using a flow rate of 30 μl/min, samples were desalted on an Agilent C18 trap (0.3 × 5 mm, 5 μm) for 3 min, followed by separation on a Vydac Everest C18 (300 A, 5 μm, 150 mm × 150 μm) column at a flow rate of 1 μl/min. A gradient of 10–60% buffer B over 45 min where buffer A = 1% ACN/0.1% FA and buffer B = 80% ACN/0.1% FA was used to separate peptides. Eluted peptides were directly analysed on a Triple TOF 5600 instrument (ABSciex) using a Nanospray III interface. Gas and voltage settings were adjusted as required. MS TOF scan across *m/z* 350–1800 was performed for 0.5 s followed by information dependent acquisition of the top 20 peptides across *m/z* 40–1800 (0.05 s per spectrum).

Proteomics data analysis

The generated data was converted to mgf format and searched in MASCOT v. 2.4.1 accessed via the Australian Proteomics Computational Facility. The data was analyzed against the SwissProt protein database with the following settings: species restriction *C. elegans* (3476 sequences), two missed cleavages, with trypsin as an enzyme, MS tolerance of 50 ppm, MS/MS tolerance of 0.1 Da, oxidation (met, variable) and carbamidomethylation (cys, fixed) modifications were also included. The Mascot search results were accepted if a protein hit included at least two significant peptide matches. For confident statistical analysis and comparison of N2 (wild type), *dld-1* suppressed worms *dld-1(wr4)*, Aβ expressing worms CL4176 with and without *dld-1* suppression, we selected only common proteins in triplicates under any experimental conditions. Using Label free quantification, emPAI values were compared for each group after quantil-quantile normalization using Solo software http://www-microarrays.u-strasbg.fr/Solo/index.html followed by inter-experimental normalization around the average.[56,57]

Functional analysis of proteomics data

Differentially expressed proteins of N2 (wild type), *dld-1* suppressed worms *dld-1(wr4)*, Aβ expressing worms CL4176 with and without *dld-1* suppression nematodes identified by MS analysis were scanned for statistically over-represented (enriched) functional categories relative to the entire proteome using the Database for Annotation, Visualization and Integrated Discovery (DAVID) (version 6.7) http://david.abcc.ncifcrf.gov/. We used Gene Ontology (GO) terms and Kyoto Encyclopedia of Genes and Genomes (KEGG) pathways for this analysis to reveal how the metabolic were affected by *dld-1* suppression.

Statistical analysis

Differences due to treatments, strains and RNAi gene suppression were analyzed for statistical significance using GraphPad prism 7.00. Paralysis curves were compared using the log-rank (Mantel–Cox) test. Pairwise treatments were analyzed for statistical significance by independent student's t-test. Anova was used to compare statistical difference among 3 or more groups. A *P* value less than 0.05 was considered statistically significant.

Results

The effect of metabolic rate on Alzheimer's disease is an unresolved issue. While a decline in respiration rate is associated with both age of onset and the severity of AD, there are possible alternative explanations. Meanwhile, the decrease in metabolic rate with age may trigger the age-related increase in AD; it is also possible that the change in metabolic rate is simply a response that protects against the progression of AD. We used *dld-1* gene suppression to directly test the effect of suppression of energy metabolism in several different *C. elegans* models of Aβ pathology. Specifically, we tested the effect of *dld-1* gene suppression on nematodes that express Aβ either constitutively or with temperature induction in muscle cells or constitutively throughout the nervous system. The general experimental paradigm is to expose the nematodes to conditions known to result in Aβ toxicity and to determine whether genetic suppression of *dld* activity influences that toxicity.

dld-1 suppression alleviates Aβ pathology in transgenic *C. elegans*

In our study, *dld-1* RNAi effectively suppresses the *dld-1* mRNA and subsequent protein expression as determined by real-time quantitative PCR and Western blotting, respectively. We assessed the *dld-1* mRNA and protein levels in the Aβ expressing strain CL4176 before and after *dld-1* suppression, compared to the wild type strain N2 and the *dld-1* mutant *dld-1*(*wr4*). When the *dld-1* gene was suppressed by RNAi, both transcript and protein decreased to the levels in the *dld-1*(*wr4*) mutant (Fig. 1A and B).

dld-1 suppression alleviates Aβ pathology in transgenic *C. elegans*

Transgenic expression and deposition of Aβ in body wall muscle cells of *C. elegans* causes severe, age-progressive paralysis. A temperature shift to 25 °C was used to induce high level expression of Aβ. Fewer than 10% of the nematodes of the CL802 control strain that lacks the human Aβ transgene were paralyzed by 38 h, i.e., unresponsive to prodding. In contrast, 100% of the worms of the CL4176 strain that does express human Aβ were unresponsive at

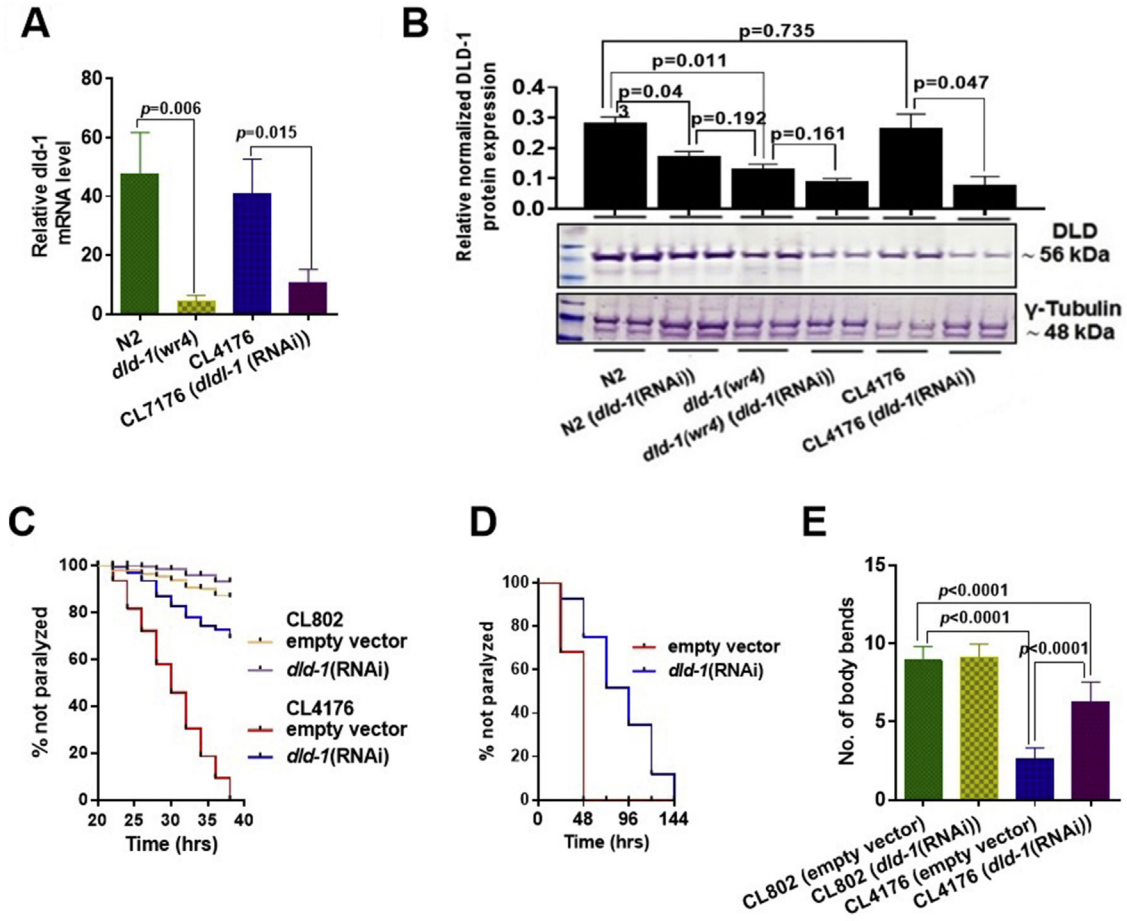

Figure 1 *dld-1* mutation, or suppression by RNAi causes a decrease in *dld-1* transcript and protein levels and also alleviates paralysis due to human Aβ expressed in transgenic *C. elegans*. Synchronized L1 stage worms of the Aβ expressing strain CL4176 were fed *E. coli* that expressed *dld-1* dsRNA for 36 h at 16 °C. The temperature was raised to 25 °C for 36 h to enhance Aβ expression. Temperature was also increased to 25 °C in control worms (N2 and *dld-1*(*wr4*)) that do not express Aβ peptide. (**A**) Results of real-time quantitative PCR from three independent trials ($n = 200$ for each experiment) showing a significant decrease in *dld-1* mRNA expression in *dld-1* mutated and suppressed worms. (**B**) Western blot of protein extracted from cell lysate. Anti-lipoamide dehydrogenase antibody (ab133551) was used to detect DLD protein, whereas anti-γ-tubulin antibody (ab50721) was used as reference control and normalizing factor. Time-dependent paralysis of the Aβ-expressing strain CL4176, with and without *dld-1* RNAi. Paralysis of synchronized L1 worms was measured on NGM plates seeded with *E. coli* strain HT115 containing either empty vector or a *dld-1* RNAi construct. After 36 h at 16 °C, the temperature was up-shifted to 25 °C. Paralyzed worms were counted 24 h after the temperature shift and thereafter, every 2 h. (**C** & **D**) Extended time-dependent paralysis analysis. As *dld-1* RNAi significantly delayed paralysis, we repeated the analysis but monitored the worms every 24 h until the last worm become paralyzed. Kaplan—Meyer survival curves were compared using a Log-rank test. (**E**) CL4176 worms were synchronized and placed on plates either seeded with *E. coli* strain HT115 containing either empty vector or a *dld-1* RNAi construct. After 36-h incubation at 16 °C, the temperature was increased to 23 °C for 36 h. Worms were collected, washed and transferred to fresh plates. Worms were touched at the head region with a platinum wire and total number of body bends were counted under the microscope at 20 °C. Quantification of the DLD bands from Western blots using GelQuantNET software. Graphs and Western blots represent the results from three independent experiments. Errors bars = mean ± SD. Results represented data from three independent trials ($n = 40$—60 worms/trial). Bars = mean ± SD.

38 h (Fig. 1C). Suppression of *dld-1* in CL4176 reduced the frequency of paralysis due to Aβ expression to only ~30%, whereas suppression of the *dld-1* gene did not alter the robust activity of the control strain, CL802. When we extended the time of the assay (Fig. 1D), we found that CL4176 worms in which *dld-1* gene expression had been suppressed did not become completely paralyzed until 144 ± 24 h. We repeated the test on CL2006 worms in which Aβ is expressed constitutively and found that suppression of the *dld-1* gene also delayed paralysis in these worms (Fig. S1). Thus, *dld-1* gene suppression prevents, to a large degree, the pathology associated with Aβ that causes paralysis.

Due to its participation in key steps of energy metabolism, *dld-1* suppression could result in a decrease in both glycolysis and the TCA cycle and therefore ATP production. We attempted to mimnic the effect of *dld-1* gene suppression by the addition of a non-metabolisable glucose

analogue, 5 mM 2-deoxy-D-glucose that does not feed metabolites into the TCA cycle, thereby decreasing oxidative phosphorylation. We found that this compound to the growth medium also caused a decrease in *dld-1* mRNA and DLD protein expression, leading to protection against Aβ-mediated paralysis in mutated worms (Fig. S2).

A second movement assay was performed that involved tapping the worms with a platinum wire and counting the number of body bends for 30 s. The worms were prepared as for the preceding assay except that the assay was carried out at room temperature (20 °C) immediately after a 36 h temperature induction of Aβ expression at 23 °C. We found that as with the immobility assay, expression of human Aβ in the CL4176 strain resulted in a decrease in the rate of movement. Suppression of the *dld-1* gene by RNAi significantly improved mobility of CL4176 worms expressing human Aβ, resulting in 6.2 ± 1.3 rather than 2.6 ± 0.7 body bends ($P < 0.0001$) (Fig. 5E). The control CL802 worms that did not contain the Aβ transgene were unaffected by *dld-1* suppression (9.1 ± 0.8 rather than 8.9 ± 0.9 body bends) ($P = 0.529$).

Expression of Aβ in muscle cells inhibits acetylcholine (ACh) neurotransmission, which may be related to the observation that ACh agonists are commonly used to delay the symptoms of Alzheimer's disease.[58] The inhibition of cholinergic neurotransmission by Aβ can be conveniently assayed by the protection it provides against a normally toxic dose of cholinergic agonist. Thus, restoration of normal sensitivity to the agonist is an indication of a decrease in the neurotoxic effects of Aβ. To check whether *dld-1* inhibition restores normal ACh neurotransmission in CL2006 worms that constitutively express Aβ in muscle, we monitored paralysis in response to the cholinergic agonists, aldicarb (a potent acetylcholinesterase inhibitor) and levamisole (a cholinergic receptor agonist).

Resistance of the CL2006 strain to ACh agonists is due to production and deposition of both Aβ oligomers and fibrils.[59] Exposure to aldicarb (Fig. 2A) results in paralysis within 180 min, which, as expected, occurs more rapidly under *dld-1* gene suppression (within 120 min, $P = 0.0001$). Similarly, paralysis in response to levamisole is decreased from 240 min to 150 min (Fig. 2B) when the *dld-1* gene is suppressed by RNAi ($P = 0.0001$). Unlike the response in strains in which Aβ is expressed, suppression of *dld-1* had no effect on the response to either aldicarb or levamisole in either wild type or *dld-1* mutant worms (Fig. S3). Both non-transgenic strains became paralyzed earlier than transgenic worms that express Aβ (~120 min for both aldicarb and levamisole). Our results indicate that *dld-1* suppression restores near normal ACh neurotransmission in Aβ expressing worms via a decrease in Aβ-toxicity.

Additional assays have been developed to monitor the toxicity of Aβ that is expressed in neurons; impaired chemotaxis, hypersensitivity toward serotonin (5-HT), and reduced fecundity and egg hatching.[43,60] Neural expression of Aβ in strain CL2355 significantly impaired chemotaxis toward benzaldehyde (chemotaxis index = 0.05 ± 0.01) relative to the non-Aβ control strain CL2122 (CI = 0.20 ± 0.02, $P = 0.002$) (Fig. 2C). Whereas suppression of the *dld-1* gene did not affect chemotaxis of the control strain (CI = 0.22 ± 0.02, $P = 0.4$), it significantly improved chemotaxis of strain CL2355 (CI = 0.14 ± 0.01, $P = 0.002$). While the chemotaxis index was improved by suppression of the *dld-1* gene in Aβ expressing worms, it did not fully restore chemotaxis to control levels ($P = 0.02$).

Serotonin is an important biogenic amine neurotransmitter that mediates locomotion, egg laying and feeding behaviour in *C. elegans*. Exogenously applied serotonin causes paralysis in worms, which is exacerbated by expression of human Aβ.[43] In our study, 64 ± 4% of worms of the control strain CL2122 were active after exposure to 1 mM serotonin for 5 min, but this was reduced to 27 ± 3% in the CL2355 strain that constitutively expresses Aβ throughout the nervous system ($P = 0.002$). Suppression of the *dld-1* gene did not affect the activity of the control strain CL2122 (57 ± 7%, $P = 0.3$), but could partially alleviate serotonin induced paralysis in CL2355, increasing the percentage of worms that were active to (49 ± 6%, $P = 0.004$) but not to the level of the no-Aβ control strain ($P = 0.03$) (Fig. 2D).

Serotonin and ACh neurotransmission control egg laying,[61] an activity that is inhibited by neuronal expression of Aβ. Based on our findings above, we reasoned that suppression of the *dld-1* gene would reverse the negative effect of Aβ expression on fecundity. Aβ expression significantly reduced egg laying in CL2355 relative to the control strain, CL2122 (157 ± 8 vs 273 ± 23, $P = 0.001$). While there was no significant effect of *dld-1* gene suppression by RNAi on the strain that did not express Aβ (273 ± 23 vs 261 ± 19, $P = 0.5$), suppression of the *dld-1* gene caused a marked improvement in fecundity in CL2355 (157 ± 8 vs 207 ± 11, $P = 0.002$). The improvement in fecundity did not reach that of the matched CL2122 control ($P = 0.01$) (Fig. 2E).

Aβ expression also negatively affects egg hatching, with 61.8% of CL2355 eggs remaining un-hatched after 24 h. In contrast, only 14.2% of CL2122 eggs remained unhatched. Inhibition of *dld-1* resulted in a significant decrease in unhatched eggs after 24 h, 30.5% (Fig. 2F). The same trend persisted over the next two days. There was no effect of *dld-1* suppression on egg hatching of the control strain CL2122.

dld-1 suppression reduces Aβ protein oligomerization without affecting Aβ peptide levels

A reduction in Aβ toxicity in our study could result from either a decrease in overall Aβ peptide levels or a decrease in the formation of toxic Aβ oligomers.[62] We did not observe any significant change in Aβ mRNA levels after *dld-1* gene suppression, indicating that gene expression was not affected (Fig. 3A). We then assessed whether *dld-1* gene suppression affected either the total amount of Aβ peptide produced or the degree of Aβ oligomerization. We found no change in the overall level of Aβ peptide due to *dld-1* gene suppression (Fig. 3B and C). However, there was a significant decrease in the proportion of Aβ peptide in the form of ~19 kDa oligomers and a corresponding increase in ~4 kDa monomers (0.31 ± 0.13 vs 0.71 ± 0.023, $P = 0.045$) when the *dld-1* gene was suppressed in strain CL4176 (Fig. 3B and D). In contrast, there was no significant change in oligomers of 12 kDa, 16 kDa or 23 kDa.

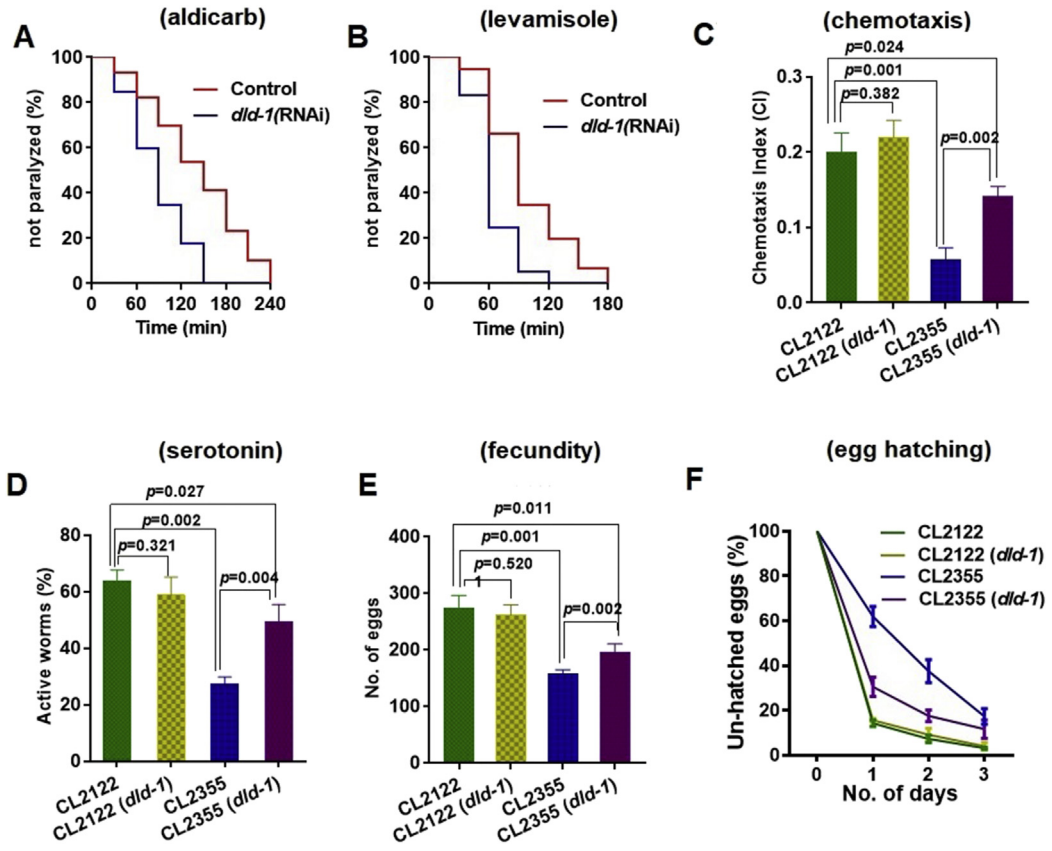

Figure 2 Effect of *dld-1* suppression on impaired behaviour in *C. elegans* that express Aβ in neurons. (**A, B**) Acetylcholine neurotransmission assay in worms that express Aβ in muscle. Paralysis assay show that *dld-1* gene suppression improves acetylcholine neurotransmission in constitutive Aβ expressing *C. elegans* strain CL2006. (**A**) Time-dependent paralysis transgenic worms fed on aldicarb (1 mM) with and without *dld-1* RNAi. (**B**) Time-dependent paralysis of worms fed on levamisole (0.2 mM) with and without *dld-1* RNAi. Results represented data from three independent trials ($n = 40–60$ worms/trial). Assay curves were compared using Log-rank test. Results represent the average of three independent trials. (**C**—**F**) Chemotaxis, 5-HT serotonin sensitivity and, egg laying and hatching were compared between a no-Aβ control (CL2122) and that express Aβ in neurons (CL2355). Synchronized worms were fed with *E. coli* containing either empty vector or a vector that expresses *dld-1* dsRNA. (**C**) Analysis of chemotaxis behaviour in worms that express Aβ in neurons. Synchronized worms were placed at 16 °C for 36 h, and then shifted to 25 °C. L4 worms were collected and assayed for chemotaxis towards benzaldehyde at room temperature ($n = 40–50$ worms in each well/trial). (**D**) Evaluation of serotonin sensitivity in worms that express Aβ in neurons. Synchronized L4 stage worms were assessed for serotonin hypersensitivity at room temperature by placing them in a 96 well plate containing 250 μl of 1 mM serotonin ($n = 25–30$ worms/trial) and counted for paralysis after 5 min. Three independent trials were run for each experiment. (**E**) Fecundity of worms that express Aβ in neurons with or without *dld-1* RNAi. (**F**) Time course of egg hatching percentage in worms that express Aβ in neurons. For Fig. 3C and D, worms were synchronized and placed at NGM plates with or without *dld-1* RNAi at 16 °C until L4 stage appeared. Ten L4 stage worms were picked to fresh plates at 23 °C to induce transgene expression. After 24 h at 23 °C, adults were removed. Plates were shifted to 20 °C for remaining assay and eggs and larvae were counted each day for 3 days. Total number of eggs were estimated by adding the total number of un-hatched eggs and larvae present. Three independent trials were run for each experiment. Bars = mean ± SD.

dld-1 gene suppression reduces ROS burden

Another possible mechanism whereby *dld-1* gene suppression might reduce the toxicity of Aβ is via a decrease in levels of reactive oxygen species, as ROS can induce aggregation of Aβ.[14,63–65] DLD itself can generate significant amounts of ROS (superoxide), so suppression of DLD activity could lead to a decrease in superoxide production.[66,67] The superoxide dismutase-3 enzyme (SOD-3) converts superoxide into O_2 and H_2O_2. Because the *sod-3* gene is induced by its substrate, superoxide, we used a strain of *C. elegans* (CF1553) that expresses GFP under the control of the *sod-3* promoter to indirectly determine the effect of *dld-1* suppression on intracellular superoxide levels. Suppression of the *dld-1* gene resulted in a decrease in GFP signal (Mean fluorescent intensity: 28,120.3 ± 7884.3 vs 16,662.8 ± 6145.7, $P = 0.0016$) (Fig. 4A).

To further elaborate our observation, we measured the cellular reactive oxygen and reactive nitrogen levels (RO/NS) levels using DCF-DA. Our results showed (Fig. 4B) that *dld-1* mutant worms have lower RO/NS levels when

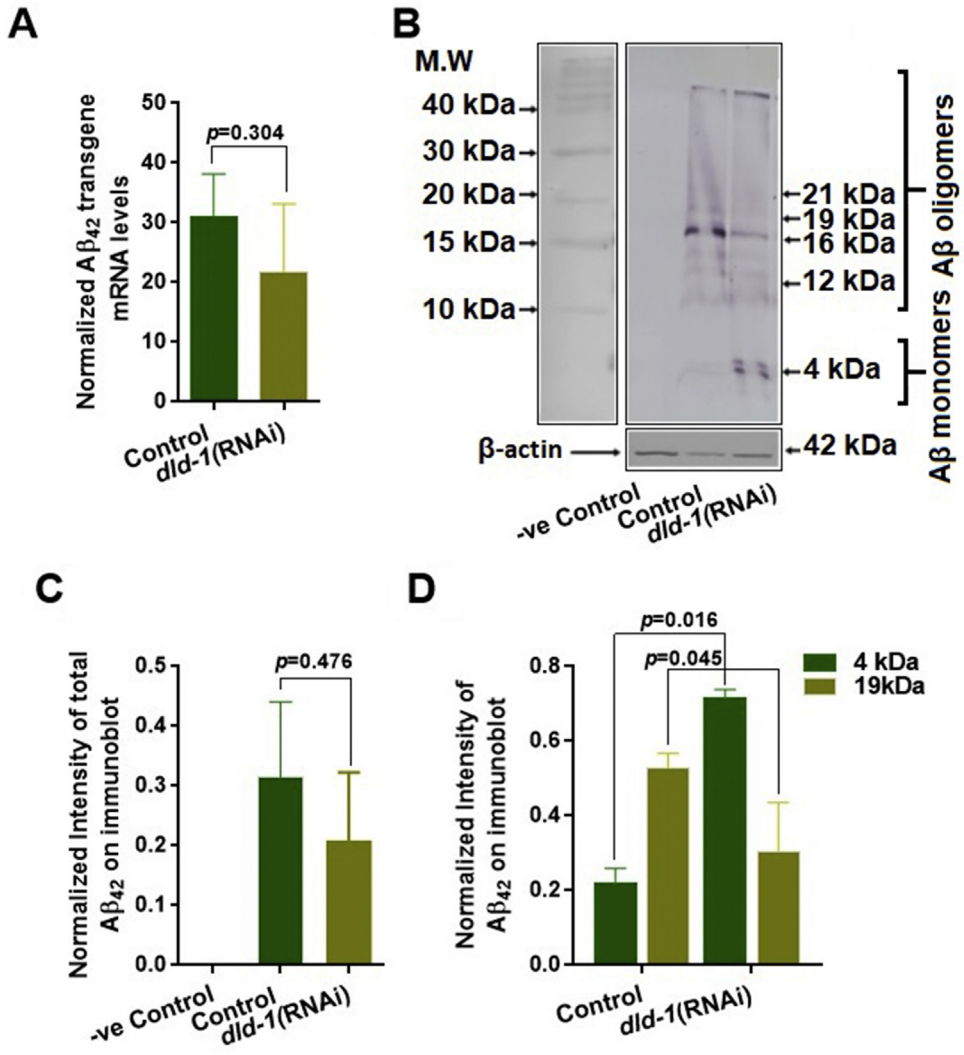

Figure 3 Effect of *dld-1* suppression on *Aβ* transgene and protein expression. (**A**) Quantitative RT-PCR of Aβ mRNA levels synchronized worms were fed with *E. coli* containing either empty vector or a vector that expresses *dld-1* dsRNA. Worms were incubated for 36 h at 16 °C and then temperature was shifted to 23 °C for further 36 h before worms were collected for RNA or protein extraction. Levels of *Aβ* mRNA are normalized to glyceraldehyde-3-phosphate dehydrogenase (*gpd-2*) transcript levels, with experiments replicated three times. (**B**) A Western blot of total soluble protein run on a 16% Tris-tricine gel shows multimers of Aβ *in C. elegans* strains expressing human Aβ. Approximate molecular weights were calculated using Novex sharp pre-stained protein standard LC5800 (Invitrogen). Arrows indicate the presence of *Aβ* monomers at 4 kDa, and oligomers at 12 kDa, 16 kDa, 19 kDa and 23 kDa. (+) *dld-1* indicates treatments in which the *dld-1* gene has been suppressed by RNAi. The control using an anti-actin antibody (ab14128) is shown below to indicate the relative amount of protein loaded onto each lane. (**C**) Densitometry of overall protein bands appeared on Western blot of each column to estimate differences in Aβ protein expression after *dld-1* suppression. (**D**) Quantification of the intensity of 4 kDa monomer and 19 kDa oligomer bands with and without *dld-1* suppression from three independent trials. Quantification was carried out using GelQuantNET software. Bars = mean ± SD.

compared to wild-type (RFU: 3455 ± 322 *vs.* 4527 ± 472, $P = 0.001$). *dld-1* gene suppression significantly decreased the RO/NS levels in the worms regardless of genotype. Thus, *dld-1* gene suppression not only decreased the RO/NS levels in the wild type (RFU: 4527 ± 472 *vs.* 2359 ± 329, $P < 0.0001$) and Aβ expressing strains (5266 ± 883 *vs.* 1675 ± 262, $P < 0.0001$), but also in the *dld-1* mutant (RFU: 3455 ± 322 *vs.* 2023 ± 395, $P < 0.001$). Interestingly, we observed no difference of RO/NS levels between the wild type and Aβ expressing strain CL4176 (RFU: 4527 ± 472 *vs.* 5266 ± 833, $P = 0.109$).

As described earlier, DLD is a major source of superoxide, which is readily converted into hydrogen peroxide (H_2O_2). Quantification of H_2O_2 could be a good indicator of DLD activity and oxidative stress as well. Although DCF-DA has been previously used for H_2O_2 measurement, recent data showed that DCF-DA does not react with H_2O_2 to form a fluorescent product, and hence cannot be used for H_2O_2 quantification.[68] To overcome this limitation, we measured the H_2O_2 levels in worm extracts spectrophotometrically (Fig. 4C). Suppression of the *dld-1* gene significantly lowers the H_2O_2 levels in the wild type strain (17.5 ± 1.2 *vs.*

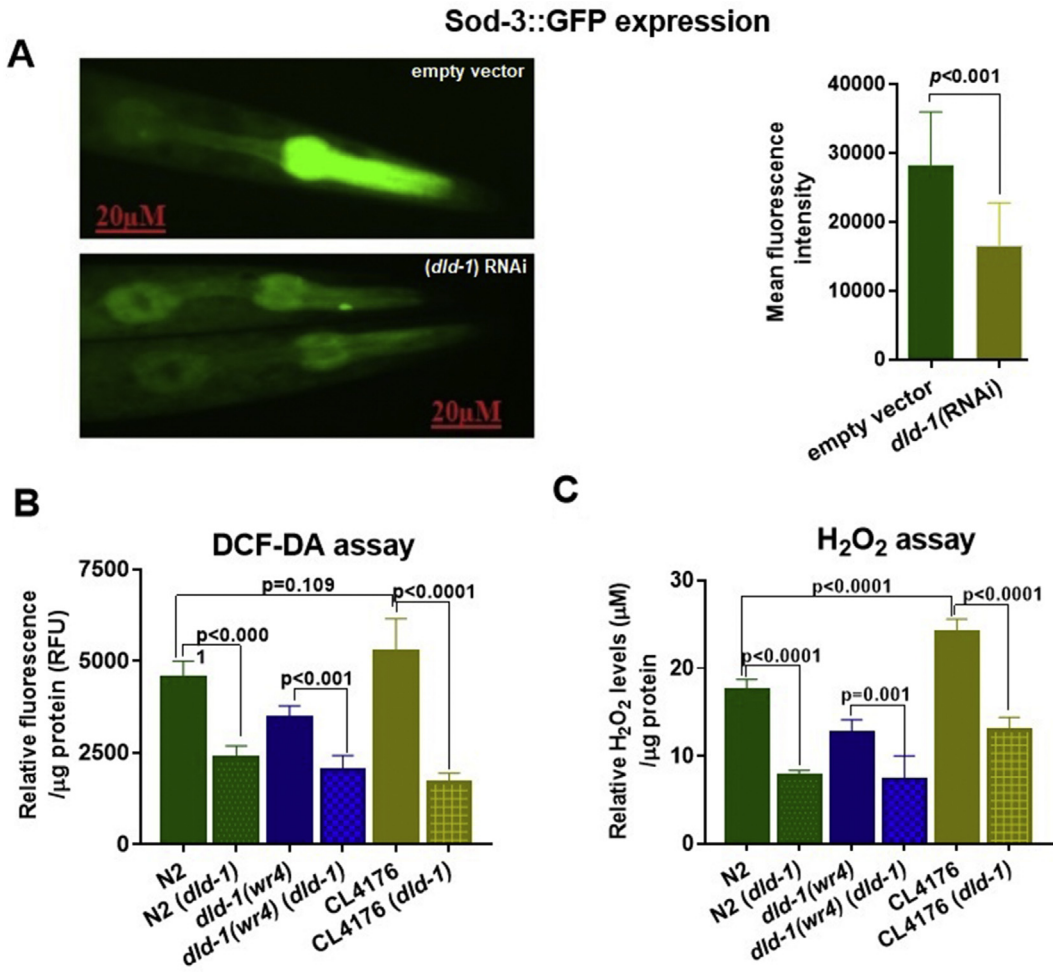

Figure 4 Suppression of the *dld-1* gene lowers the response to superoxide and lower RO/NS burden in *C. elegans*. (**A**) Synchronized L1 worms of strain CF1553 that expresses *sod-3*::gfp was fed *E. coli* containing either empty vector or vector that expressed *dld-1* ds-RNA for 72 h at 20 °C. GFP fluorescence was quantified in at least ten worms from each group using ImageJ. Mean fluorescence intensity was measured using the formula; Mean fluorescence intensity = Integrated density − (area of selected worm × mean fluorescence of background readings). (**B**) Measurement of RO/NS levels in worms using DCF-DA. Results are given as relative fluorescent intensity units (RFU) after normalizing the mean intensities by total protein levels. (**C**) Measurement of H_2O_2 levels in worms. Worms were synchronized and placed on NGM plates seeded with *E. coli* containing empty vector or expressing *dld-1* ds-RNA. Bars = mean ± SD.

7.8 ± 0.6 μM, $P < 0.0001$), the *dld-1* mutant (12.5 ± 1.6 *vs.* 7.3 ± 2.6 μM, $P = 0.001$) and Aβ expressing worms (24.1 ± 1.4 *vs.* 12.9 ± 1.5 μM, $P < 0.0001$). We observed higher H_2O_2 levels in wild type when compared to the *dld-1* mutant (17.5 ± 1.2 *vs.* 12.5 ± 1.6 μM, $P < 0.001$). It is worth noting that H_2O_2 levels were significantly higher in Aβ expressing worms than wild-type (17.5 ± 1.2 *vs.* 24.1 ± 01.4 μM, $P < 0.0001$).

Protective effect of *dld-1* suppression is not associated with energy depletion

DLD is a core enzyme of oxidative respiration and the *dld-1*(*wr4*) mutation is known to inhibit energy metabolism.[51] FCCP is also a disruptor of mitochondrial energy metabolism, but it acts in quite a different manner. Both likely disrupt the generation of ATP, but by opposite mechanisms. DLD disruption slows the flow of metabolites through the TCA cycle, thereby restricting the delivery of electron to the electron transport chain via NADH. FCCP dissipates the proton gradient established by the electron transport chain. Thus, while FCCP triggers a compensatory acceleration in the flow of electrons, much of the effort is futile, resulting in a decrease in ATP synthesis. Given the strikingly different mechanisms of action but the common end result, we sought to determine whether FCCP, like *dld-1* gene suppression, was capable of protecting against Aβ-induced toxicity. To accomplish this, we measured Aβ-mediated toxicity in combination with either *dld-1* gene suppression or exposure to 17.5 μM FCCP or both (Fig. 5A). Suppression of the *dld-1* gene alone had no negative impact on survival of any strain and provided protection against Aβ in strain CL4176, decreasing mortality from 20.5% ± 4.2—8.2% ± 5.3, $P = 0.004$).

Exposure to FCCP had an effect very different to that of *dld-1* gene suppression. The dose of FCCP that was used

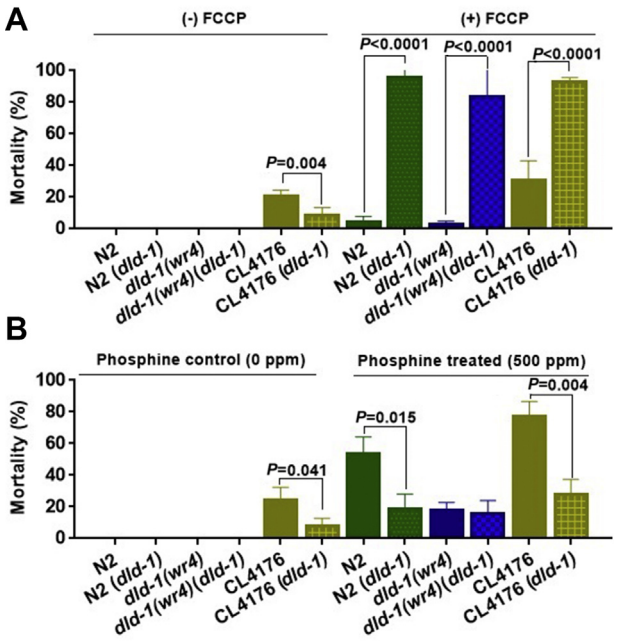

Figure 5 Effect of *dld-1* suppression in the presence of FCCP and/or phosphine on worms expressing Aβ. (**A**) Mortality assay of *C. elegans* treated with the mitochondrial uncoupler FCCP. When the *dld-1* gene was suppressed in the presence of 17.5 μM uncoupler, the compounded disruption of energy metabolism resulted in high level mortality in each of the three strains regardless of the presence of the Aβ peptide ($n = 50-100$ for each experiment). Three independent trials were run. Bars = mean ± SD. (**B**) Suppression of the *dld-1* gene protects against the toxicity of phosphine independent of Aβ presence. *dld-1* gene mutation, or suppression of the *dld-1* gene by RNAi, reduced mortality caused by 500 ppm phosphine in both wild type (N2) and Aβ-expressing worms of strain CL4176. Three independent trials were run ($n = 50-80$ for each trial). Bars = mean ± SD.

caused negligible mortality on its own, but rather than providing protection against Aβ-mediated mortality, it produced an apparent, but not significant increase in mortality from 20.5% ± 4.2—30.8% ± 12.3 ($P = 0.107$). This lack of protection by FCCP shows that protection against Aβ cannot be attributed to a decrease in the efficiency ATP generation, but neither was it negatively affected by the required increase in metabolic flux required to maintain ATP levels required for survival. Mortality caused by Aβ increases greatly when *dld-1* gene suppression by RNAi is combined with exposure to FCCP, thus, exposure to FCCP alone caused 30.8% ± 12.3 mortality, whereas *dld-1* gene suppression combined with exposure to FCCP resulted in mortality of 92.9% ± 2.8, $P < 0.0001$). The increase in mortality was not restricted to the Aβ-expressing transgenic strain, however, but also was observed in the wild-type N2 strain (4.2% ± 3.5 *vs.* 95.7% ± 4.1, $P < 0.0001$) and the *dld-1*(*wr4*) mutant (3.7% ± 3.3 *vs.* 83.2% ± 16.8, $P < 0.0001$). The most likely explanation is that the decrease in metabolite flux due to a decrease in DLD containing metabolic complexes, together with futile pumping of protons across the inner mitochondrial membrane caused by FCCP, results in a crisis of energy metabolism that affects all three strains equivalently, and that this is largely independent of whether Aβ peptide is expressed. The effect of the combined treatment clearly indicates that the dose of FCCP that was used was having an underlying biological effect, despite the rather benign response to FCCP exposure on its own.

dld-1 suppression provides protection independently against Aβ and phosphine toxicity

The *dld-1*(*wr4*) mutation that is used in the current study confers resistance against phosphine toxicity,[69] a phenotype that can also be achieved by *dld-1* gene suppression.[39] Phosphine is a fumigant that induces ROS production and lipid peroxidation but causes decreased respiration rates as well as a reduction in mitochondrial membrane potential and ATP levels.[70] Thus phosphine, like Aβ, impairs mitochondrial function, causing phenotypes that are countered by *dld-1* inhibition. Due to these similarities, we investigated interactions between *dld-1*, phosphine and Aβ.

We found that exposing Aβ expressing transgenic worms to 500 ppm phosphine (the LC_{50} of wildtype *C. elegans*) for 24 h, followed by 48 h of recovery at room temperature, increased the mortality of the wildtype N2 strain to the same degree as the Aβ expressing strain CL4176 (Fig. 5B). Thus, mortality of N2 increased from 0% to 48.5 ± 10.7% in response to 500 ppm phosphine and mortality of CL4176 increased from 22.9 ± 7.8% to 75.6 ± 9.9%. The resistance phenotype of the *dld-1*(*wr4*) mutant was unaffected by RNAi-mediated suppression of the *dld-1* gene, indicating that the mutation and gene suppression confer resistance to phosphine by the same mechanism. The phosphine toxicity and Aβ toxicity are simply additive, regardless of whether or not the *dld-1* gene is suppressed. This indicates that while both phosphine and Aβ toxicity can be modulate by manipulating the DLD enzyme, they are mediated independently without any interaction. Similar findings were observed when we treated the worms at a higher phosphine concentration of 2000 ppm (Fig. S4).

dld-1 suppression resulted in metabolic regulation as well as pathways involved in longevity and stress response

Being a core metabolic enzyme, suppression of *dld-1* could result in remodeling of metabolic as well as other pathways. Proteomics analysis was performed to determine the impact of *dld-1* suppression on metabolism and other associated pathways. Although we performed proteomics analysis on whole solubilized proteins, we restricted the present results to genes/proteins involved only in metabolism or closely associated pathways. The extracted proteins were analyzed using LC-MS/MS to interpret the differential regulation of proteins after *dld-1* suppression or in *dld-1* knock downed worms. Although we preformed proteomics analysis on wild type N2, *dld-1* suppressed worms wr4 (*dld-1*), and Aβ expressing worms CL4176 with and without *dld-1* suppression, here we somehow restricted our results to only Aβ expressing worms. Post-MS analysis revealed that out of 467 differentially regulated proteins among all groups, 104 proteins belong to

metabolic or closely associated pathways (Fig. 6A and supplementary data). As stated earlier, we restricted our further analysis to only proteins that were differentially regulated only in Aβ expressing worms with and without *dld-1* suppression. We found 30 differentially regulated proteins that were closely associated with energy metabolism in Aβ expressing worms CL4176 with and without *dld-1* suppression (Fig. 6B).

Gene ontology (GO) and functional annotation was performed to categorize the molecular, biological and cellular functions of the differentially abundant proteins using online tools like UniProtKB, DAVID and KEGG. These analyses revealed an enrichment of GO terms including energy metabolism, such as glycolysis (4 genes: gpdh-2 ldh-1, pfk-1.1, sqv-4), TCA cycle (4 genes: *dld-1*, idha-1, mev-1, suca-1), oxidative phosphorylation (8 genes: asg-1, atp-1, cox-5A, cox-6A, fs3f4-10, ucr-1 vha-9, vha-14), amino acid metabolism (3 genes: b0250.5, gta-1, hpd-1) cell signaling (5 genes: let-92, nkb-1, nkb-3, pph-5, tomm-22), proteasomal pathways (rpn-7, rpn-12), glutathione metabolism (1 gene: rnr-2) and longevity (sod-2, hsp-110, hsp-12.2) (Fig. 6C).

Discussion

To assess the role of energy metabolism in AD-associated Aβ proteotoxicity in worms, we used RNAi to suppress the activity of the *dld-1* gene, which is known to suppress aerobic

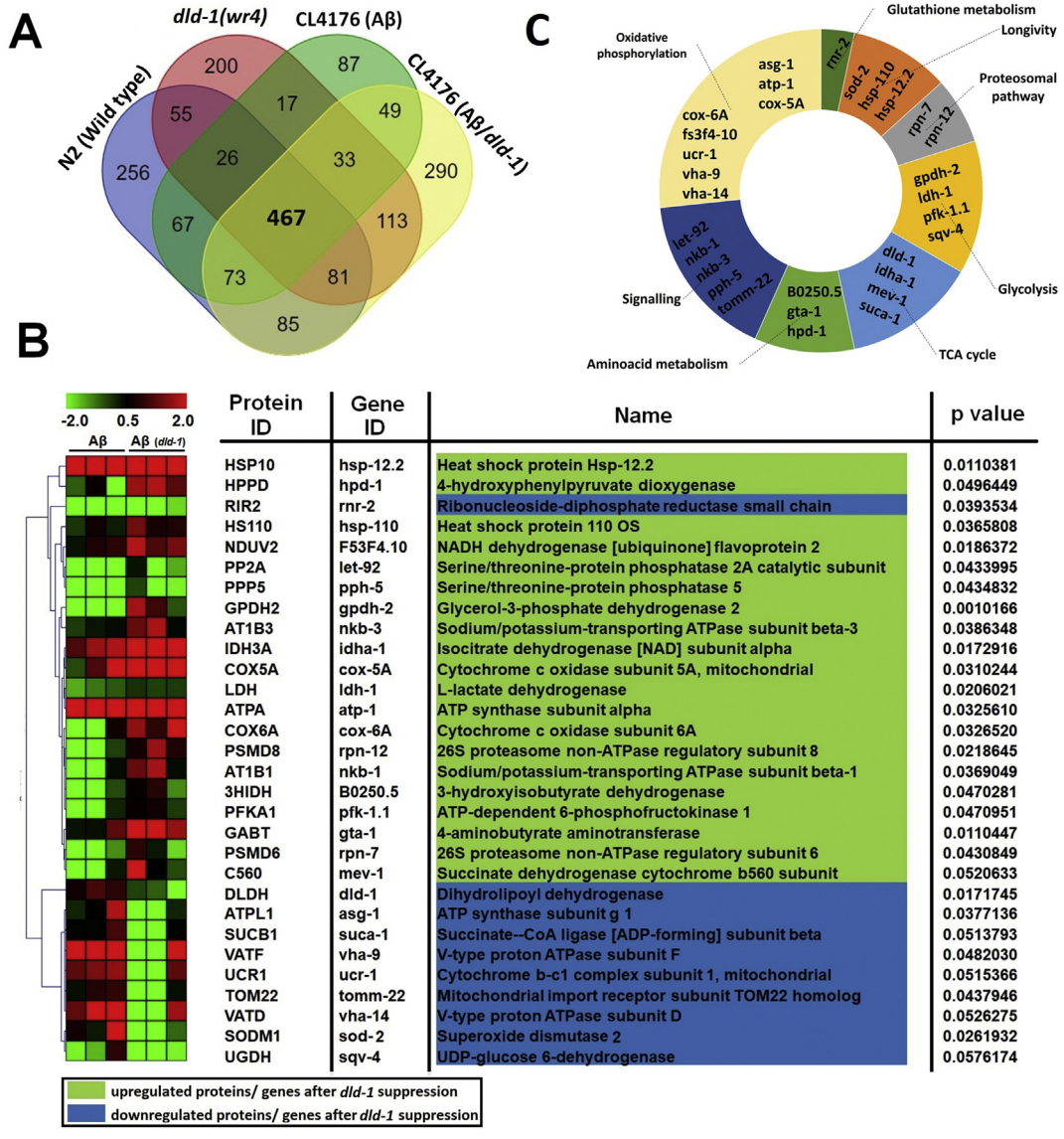

Protein ID	Gene ID	Name	p value
HSP10	hsp-12.2	Heat shock protein Hsp-12.2	0.0110381
HPPD	hpd-1	4-hydroxyphenylpyruvate dioxygenase	0.0496449
RIR2	rnr-2	Ribonucleoside-diphosphate reductase small chain	0.0393534
HS110	hsp-110	Heat shock protein 110 OS	0.0365808
NDUV2	F53F4.10	NADH dehydrogenase [ubiquinone] flavoprotein 2	0.0186372
PP2A	let-92	Serine/threonine-protein phosphatase 2A catalytic subunit	0.0433995
PPP5	pph-5	Serine/threonine-protein phosphatase 5	0.0434832
GPDH2	gpdh-2	Glycerol-3-phosphate dehydrogenase 2	0.0010166
AT1B3	nkb-3	Sodium/potassium-transporting ATPase subunit beta-3	0.0386348
IDH3A	idha-1	Isocitrate dehydrogenase [NAD] subunit alpha	0.0172916
COX5A	cox-5A	Cytochrome c oxidase subunit 5A, mitochondrial	0.0310244
LDH	ldh-1	L-lactate dehydrogenase	0.0206021
ATPA	atp-1	ATP synthase subunit alpha	0.0325610
COX6A	cox-6A	Cytochrome c oxidase subunit 6A	0.0326520
PSMD8	rpn-12	26S proteasome non-ATPase regulatory subunit 8	0.0218645
AT1B1	nkb-1	Sodium/potassium-transporting ATPase subunit beta-1	0.0369049
3HIDH	B0250.5	3-hydroxyisobutyrate dehydrogenase	0.0470281
PFKA1	pfk-1.1	ATP-dependent 6-phosphofructokinase 1	0.0470951
GABT	gta-1	4-aminobutyrate aminotransferase	0.0110447
PSMD6	rpn-7	26S proteasome non-ATPase regulatory subunit 6	0.0430849
C560	mev-1	Succinate dehydrogenase cytochrome b560 subunit	0.0520633
DLDH	dld-1	Dihydrolipoyl dehydrogenase	0.0171745
ATPL1	asg-1	ATP synthase subunit g 1	0.0377136
SUCB1	suca-1	Succinate--CoA ligase [ADP-forming] subunit beta	0.0513793
VATF	vha-9	V-type proton ATPase subunit F	0.0482030
UCR1	ucr-1	Cytochrome b-c1 complex subunit 1, mitochondrial	0.0515366
TOM22	tomm-22	Mitochondrial import receptor subunit TOM22 homolog	0.0437946
VATD	vha-14	V-type proton ATPase subunit D	0.0526275
SODM1	sod-2	Superoxide dismutase 2	0.0261932
UGDH	sqv-4	UDP-glucose 6-dehydrogenase	0.0576174

Figure 6 Differential interactions, gene ontology and expression analysis of significant genes involved in pathways associated with *dld-1* suppression in Aβ expressing worms. (**A**) Venn diagram of overlapping proteins in worm strain normally fed including wild type N2, *dld-1* knockdown strain *dld-1(wr4)*, Aβ expressing worms CL4176, and CL4176 strain fed with *dld-1* RNAi. Data include at least three biological replicates for each strain. (**B**) Expression analysis of statistically significant genes differentially regulating between Aβ control and Aβ expressing worms fed with *dld-1* RNAi. (**C**) Gene ontology profiling of differentially regulated genes in Aβ expressing worms either fed with *dld-1* RNAi or not.

respiration.[71,72] Our results show that suppression of the *dld-1* gene significantly alleviates the symptoms associated with Aβ expression in either muscles or neurons of *C. elegans*. As described earlier, knock down of dld-containing complexes may lead to deleterious effects in vertebrate models of AD, here in this study feeding with RNAi or in wr4 (*dld-1*) worms have 70–80% reduction in DLD expression when compared to wild type thus not completely shut down the activity of these complexes.

We find that suppression of the *dld-1* gene does not affect either the Aβ transgene mRNA levels or the levels of Aβ peptide. Suppression of *dld-1* does, however, significantly inhibit the oligomerization of Aβ. Accumulation of Aβ oligomers is thought to be a major culprit in AD progression,[73,74] whereas monomers actually help to maintain glucose homeostasis and are not toxic.[75,76] Our findings suggest that *dld-1* suppression reduces Aβ oligomerization thus resulting in reduced paralysis, better movement rates, and improved behavioral phenotypes as observed previously.[43,59,77,78] Both mutation and RNAi-mediated suppression of the *dld-1* gene result in phosphine resistance and an extended lifespan,[38,39,78] as well as inhibition of Aβ oligomerization and protection against Aβ-mediated toxicity as we have shown here.

Based on our understanding of the relationship between the *dld-1* gene and phosphine toxicity/resistance, we carried out several additional assays designed to compare the mechanisms of action of *dld-1* and Aβ. When we exposed the worms to 17.5 μM FCCP, it was highly toxic when the *dld-1* gene was subjected to RNAi-mediated suppression. The basis of the interaction between FCCP and *dld-1* gene suppression is unknown. FCCP does, however, deplete the mitochondrial proton gradient that is utilized for ATP synthesis, whereas the DLD enzyme generates NADH that delivers electrons to the electron transport chain that generates the proton gradient. It may be possible that the simultaneous depletion of the proton gradient by FCCP as well as the source of electrons (NADH) by suppressing the *dld-1* gene, results in a cellular energetic catastrophe. Exposure to FCCP decreases Aβ production,[79,80] which implies that ATP depletion is more important to the protection than is the mechanism that causes the decrease in ATP. As protonophores, mitochondrial uncouplers also lower the pH of the mitochondrial matrix. At low pH, the dehydrogenase activity of DLD is inhibited and the reverse activity (diaphorase) is induced.[81,82] This would have the same effect on cellular energy metabolism as described in the previous paragraph and indeed, both mechanisms may contribute to the synergistic increase in mortality that is observed when uncoupler and *dld-1* gene suppression are combined.

We also exposed the worms to the fumigant phosphine, a mitochondrial poison that causes oxidative stress and inhibits respiration, likely by targeting the DLD enzyme.[39,70] When combined, Aβ expression and exposure to phosphine cause an additive increase in mortality. Suppression of the *dld-1* gene provides protection against both Aβ and phosphine individually and provides the same degree of protection against each of the two stressors when they are applied in combination. The similarities that we observe between the toxicity of Aβ and phosphine are worth noting. Both cause suppression of energy metabolism and yet are protected by suppression of the *dld-1* gene, a manipulation that likewise suppresses energy metabolism. The toxicity of both Aβ and phosphine is synergistically exacerbated by co-exposure to the mitochondrial uncoupler, FCCP. However, co-exposure to Aβ and phosphine results in an additive rather than synergistically increased toxicity. One interpretation of these results is that the two stressors act through the same mechanism(s), with each stressor simply increasing the magnitude of the insult.

Aβ proteotoxicity and oxidative stress are positively correlated[65,83,84] and DLD inhibition is known to reduce ROS generation.[66,85,86] We found reduced levels of the mitochondrial superoxide detoxifying enzyme SOD-3 after *dld-1* gene suppression, confirming that suppression of *dld-1* does indeed decrease the burden of ROS in *C. elegans*. The DLD enzyme and mitochondrial electron transport chain (ETC) are both major sources of ROS generation,[67,87] so the decrease in ROS production could either be direct (less ROS emanating from DLD) or indirect (less NADH feeding electrons to the ETC).

Being a part of the four core metabolic enzyme complexes and a moon lightening enzyme make *dld-1* very critical.[88] Any change in *dld-1* activity may result in impairment of energy metabolism and/or other pathways. Post proteomics analysis revealed that out of 30 differentially regulated proteins/genes, 19 belongs to energy metabolism (Fig. 6). These results show the importance of *dld-1* in regulating energy metabolism. Our results showed that *dld-1* suppression resulted in change in expression of several enzymes associated with glycolysis, TCA cycle and oxidative phosphorylation (Fig. 7). It could be possible that downstream suppression of *dld-1* may result in induced glycosylation and reduced oxidative phosphorylation according to demand-supply chain. It was interesting to show that *dld-1* suppression resulted in induced expression of genes involved in glycosylation. However, at the same time it induces expression of lactate dehydrogenase; an enzyme involved in lactic acid buildup. Induced lactic acid might be neuroprotective however, demand more research on this.[89] The *dld-1* suppression also reduces the expression of gene involved in UDP-glucoronate and glucosamine glycans production (GAGs). Reduction of GAGs in amyloid containing tissues may reduce amyloid fibril formation and destabilization.[90]

Suppression of *dld-1* resulted in induced expression of genes involved in amino acid metabolism. This could be due to decrease in nutrient supply via glycolysis to TCA cycle. Induced mev-1 levels after *dld-1* suppression may indicate lower nutrient supply for ETC. Moreover, *dld-1* suppression did not affect all the TCA enzymes and suggested a specific disruption of TCA enzymes. Reduction in expression of complex-III and complex V enzymes especially ucr-1 after *dld-1* suppression may result in reduction in ATP production. It is worth to note that Aβ has been found to interact with human ucr-1 and may results in impaired ucr-1 functions.[91] Induced expression of f53f4.10 and mev-1 genes in ETC also indicate reduced nutrient(s) supply after *dld-1* suppression. An interesting finding was induction of complex-IV enzymes cox-5A and cox-6A gene expression in Aβ expressing worms after *dld-1* expression. It has been shown that knockdown of cox-5A and cox-6A may lead to neuronal death in animal models. In a recent study, the

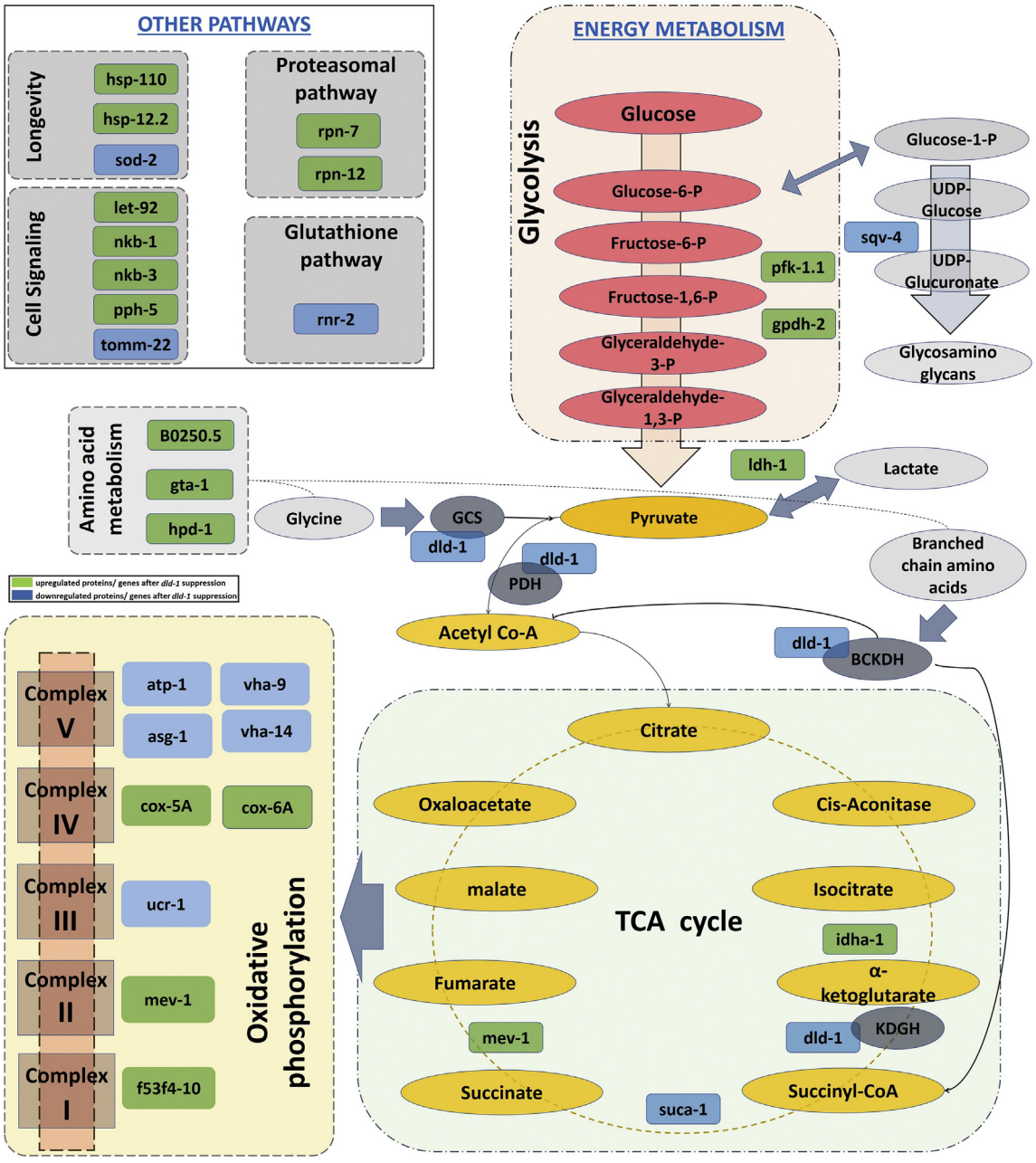

Figure 7 Schematic diagram of energy metabolism showing genes/proteins differentially regulated after *dld-1* suppression in Aβ expressing worms CL4176. Green and blue boxes indicate upregulated and down regulated genes/proteins after *dld-1* suppression. The suppression of *dld-1* after RNAi feeding resulted in differential regulation of gene/proteins in major energy metabolic and associated pathways including glycolysis, TCA cycle, oxidative phosphorylation, amino acid metabolism, cell signaling, longevity, proteasomal and glutathione pathways.

over expression of cox-6B resulted in neuronal protection by decreasing Ca^{2+} and apoptosis, and increasing cell viability.[92] Overall, these finding suggest that *dld-1* suppression only affect selective enzymes levels of energy metabolism that could be beneficial against Aβ toxicity in *C. elegans*.

Despite changes in expression of several energy metabolism enzymes, we found induced expression enzymes associated with cell signaling, glutathione pathway, proteasomal activity and longevity. Inactivation of tomm-22 levels after *dld-1* suppression may cause disruption of mitochondrial proton gradient and collapse of ETC.[93] This mechanism may explain the death of *dld-1* suppressed worms after FCCP exposure as discussed before. Meanwhile increased expression of protein-phosphatases (let-92 and pph-5) and sodium/potassium transporting ATPase subunits (nkb-1 and 3) in our study may be associated with low Aβ-toxicity after *dld-1* suppression as Aβ was found to reduced their functions after binding with them.[94–97] Decline in proteasomal activity in neurodegeneration has been well

known. Upregulation of proteasomal-associated genes in *dld-1* suppressed worms may lead to reduction in Aβ burdens.[98,99]

Suppression in *dld-1* also affected the expression of genes associated with longevity in worms. In our and a previous study, it has been shown that reduction in *dld-1* results in induced lifespan in *C. elegans*. Here in this study, *dld-1* suppression resulted in reduced expression of sod-2. Deletion of sod-2 has been associated with long lifespan in worms.[100] We may speculate that induced lifespan after *dld-1* suppression may be linked to sod-2 reduction. In this study we found that *dld-1* suppressed worms were resistible against toxicities like phosphine. Proteomics analysis of the data revealed the induced expression of heat shock proteins (hsp) 110 and 12.2 after *dld*-suppression. Induction of hsp not only protect cells from different toxic substances like Aβ but also induce lifespan.[101,102] Aβ has been well known for its deleterious effects on mitochondrial DNA. Reduction in ribonucleotide reductase (RNR) after *dld-1* suppression suggests decrease in mitochondrial DNA loss due to reduced Aβ activity.[103,104]

Conclusion

In summary, we find no evidence that metabolic suppression through DLD could be a risk factor for Aβ proteotoxicity. However, induced chronic lactic acid levels after DLD suppression could be deleterious. Our results do not distinguish between two possibilities; that neuroprotection is a direct effect of metabolic suppression or that it is an indirect effect resulting from decreased ROS generation. Regardless of the mechanism, our results are consistent with the hypothesis that a decrease in mitochondrial energy metabolism protects against Aβ pathogenicity, which, if also true in humans, could delay clinical dementia resulting from AD.

Authors contribution

P.E was responsible for the study design. W.A collected and analyzed the data.

Conflict of Interests

Both W.A and P.E have no interests to declare.

Funding

We thank Prof. Jurgen Goetz (Queensland Brain Institute) for his research support. The *C. elegans* strains were provided by the CGC, which is funded by NIH Office of Research Infrastructure Programs (P40 OD010440) WA was supported by a IPRS scholarship from the Australian Government and the University of Queensland.

Appendix A. Supplementary data

Supplementary data to this article can be found online at https://doi.org/10.1016/j.gendis.2020.08.004.

References

1. Huang Y, Mucke L. Alzheimer mechanisms and therapeutic strategies. *Cell*. 2012;148(6):1204—1222.
2. Vlassenko AG, Vaishnavi SN, Couture L, et al. Spatial correlation between brain aerobic glycolysis and amyloid-beta (Abeta) deposition. *Proc Natl Acad Sci U S A*. 2010;107(41):17763—17767.
3. Shoffner JM. Oxidative phosphorylation defects and Alzheimer's disease. *Neurogenetics*. 1997;1(1):13—19.
4. Mosconi L. Glucose metabolism in normal aging and Alzheimer's disease: methodological and physiological considerations for PET studies. *Clin Transl Imaging*. 2013;1(4),e10.
5. Vlassenko AG, Benzinger TL, Morris JC. PET amyloid-beta imaging in preclinical Alzheimer's disease. *Biochim Biophys Acta*. 2012;1822(3):370—379.
6. Calkins MJ, Reddy PH. Amyloid beta impairs mitochondrial anterograde transport and degenerates synapses in Alzheimer's disease neurons. *Biochim Biophys Acta*. 2011;1812(4):507—513.
7. Chen KH, Reese EA, Kim HW, Rapoport SI, Rao JS. Disturbed neurotransmitter transporter expression in Alzheimer's disease brain. *J Alzheimers Dis*. 2011;26(4):755—766.
8. Dienel GA, Cruz NF. Nutrition during brain activation: does cell-to-cell lactate shuttling contribute significantly to sweet and sour food for thought? *Neurochem Int*. 2004;45(2—3):321—351.
9. Kar S, Slowikowski SP, Westaway D, Mount HT. Interactions between beta-amyloid and central cholinergic neurons: implications for Alzheimer's disease. *J Psychiatry Neurosci*. 2004;29(6):427—441.
10. Liu Y, Liu F, Grundke-Iqbal I, Iqbal K, Gong CX. Deficient brain insulin signalling pathway in Alzheimer's disease and diabetes. *J Pathol*. 2011;225(1):54—62.
11. Lunt SY, Vander Heiden MG. Aerobic glycolysis: meeting the metabolic requirements of cell proliferation. *Annu Rev Cell Dev Biol*. 2011;27:441—464.
12. Costantini LC, Barr LJ, Vogel JL, Henderson ST. Hypometabolism as a therapeutic target in Alzheimer's disease. *BMC Neurosci*. 2008;9(Suppl 2),S16.
13. Ahmad W, Ebert PR. Metformin attenuates Abeta pathology mediated through levamisole sensitive nicotinic acetylcholine receptors in a *C. elegans* model of Alzheimer's disease. *Mol Neurobiol*. 2017;54(7):5427—5439.
14. Ahmad W, Ijaz B, Shabbiri K, Ahmed F, Rehman S. Oxidative toxicity in diabetes and Alzheimer's disease: mechanisms behind ROS/RNS generation. *J Biomed Sci*. 2017;24(1),e76.
15. Hooijmans CR, Graven C, Dederen PJ, Tanila H, van Groen T, Kiliaan AJ. Amyloid beta deposition is related to decreased glucose transporter-1 levels and hippocampal atrophy in brains of aged APP/PS1 mice. *Brain Res*. 2007;1181:93—103.
16. Hoyer S. Abnormalities of glucose metabolism in Alzheimer's disease. *Ann N Y Acad Sci*. 1991;640:53—58.
17. Hoyer S. Brain glucose and energy metabolism abnormalities in sporadic Alzheimer disease. Causes and consequences: an update. *Exp Gerontol*. 2000;35(9—10):1363—1372.
18. Hoyer S. Causes and consequences of disturbances of cerebral glucose metabolism in sporadic Alzheimer disease: therapeutic implications. *Adv Exp Med Biol*. 2004;541:135—152.
19. Hunt A, Schönknecht P, Henze M, Seidl U, Haberkorn U, Schröder J. Reduced cerebral glucose metabolism in patients at risk for Alzheimer's disease. *Psychiatr Res*. 2007;155(2):147—154.
20. Sun J, Feng X, Liang D, Duan Y, Lei H. Down-regulation of energy metabolism in Alzheimer's disease is a protective response of neurons to the microenvironment. *J Alzheimers Dis*. 2012;28(2):389—402.

21. Liang D, Han G, Feng X, Sun J, Duan Y, Lei H. Concerted perturbation observed in a hub network in Alzheimer's disease. *PLoS One*. 2012;7(7), e40498.
22. Dumont M, Stack C, Elipenahli C, et al. PGC-1alpha overexpression exacerbates beta-amyloid and tau deposition in a transgenic mouse model of Alzheimer's disease. *FASEB J*. 2014;28(4):1745—1755.
23. Brown AM, Gordon D, Lee H, et al. Testing for linkage and association across the dihydrolipoyl dehydrogenase gene region with Alzheimer's disease in three sample populations. *Neurochem Res*. 2007;32(4—5):857—869.
24. Ahmad W, Ebert PR. 5-Methoxyindole-2-carboxylic acid (MICA) suppresses Abeta-mediated pathology in *C. elegans*. *Exp Gerontol*. 2018;108:215—225.
25. Ahmad W. Dihydrolipoamide dehydrogenase suppression induces human tau phosphorylation by increasing whole body glucose levels in a *C. elegans* model of Alzheimer's Disease. *Exp Brain Res*. 2018;236(11):2857—2866.
26. Koike M, Koike K. Structure, assembly and function of mammalian alpha-keto acid dehydrogenase complexes. *Adv Biophys*. 1976:187—227.
27. Carothers DJ, Pons G, Patel MS. Dihydrolipoamide dehydrogenase: functional similarities and divergent evolution of the pyridine nucleotide-disulfide oxidoreductases. *Arch Biochem Biophys*. 1989;268(2):409—425.
28. Gibson GE, Chen HL, Xu H, et al. Deficits in the mitochondrial enzyme alpha-ketoglutarate dehydrogenase lead to Alzheimer's disease-like calcium dysregulation. *Neurobiol Aging*. 2012;33(6),e1121.
29. Gibson GE, Sheu KF, Blass JP, et al. Reduced activities of thiamine-dependent enzymes in the brains and peripheral tissues of patients with Alzheimer's disease. *Arch Neurol*. 1988;45(8):836—840.
30. Gibson GE, Zhang H, Sheu KF, et al. Alpha-ketoglutarate dehydrogenase in Alzheimer brains bearing the APP670/671 mutation. *Ann Neurol*. 1998;44(4):676—681.
31. Shi Q, Xu H, Kleinman WA, Gibson GE. Novel functions of the alpha-ketoglutarate dehydrogenase complex may mediate diverse oxidant-induced changes in mitochondrial enzymes associated with Alzheimer's disease. *Biochim Biophys Acta*. 2008;1782(4):229—238.
32. Stacpoole PW. The pyruvate dehydrogenase complex as a therapeutic target for age-related diseases. *Aging Cell*. 2012;11(3):371—377.
33. Banerjee K, Munshi S, Xu H, et al. Mild mitochondrial metabolic deficits by alpha-ketoglutarate dehydrogenase inhibition cause prominent changes in intracellular autophagic signaling: potential role in the pathobiology of Alzheimer's disease. *Neurochem Int*. 2016;96:32—45.
34. Johnson MT, Yang HS, Magnuson T, Patel MS. Targeted disruption of the murine dihydrolipoamide dehydrogenase gene (Dld) results in perigastrulation lethality. *Proc Natl Acad Sci U S A*. 1997;94(26):14512—14517.
35. Van Assche R, Temmerman L, Dias DA, et al. Metabolic profiling of a transgenic *Caenorhabditis elegans* Alzheimer model. *Metabolomics*. 2015;11(2):477—486.
36. Ahmad W. Overlapped metabolic and therapeutic links between Alzheimer and diabetes. *Mol Neurobiol*. 2013;47(1):399—424.
37. Ahmad W Dr, Shabbiri K Dr, Ahmad I. Prediction of human tau 3D structure, and interplay between O-beta-GlcNAc and phosphorylation modifications in Alzheimer's disease: *C. elegans* as a suitable model to study these interactions in vivo. *Biochem Biophys Res Commun*. 2020;528(3):466—472.
38. Cheng Q, Valmas N, Reilly PE, Collins PJ, Kopittke R, Ebert PR. *Caenorhabditis elegans* mutants resistant to phosphine toxicity show increased longevity and cross-resistance to the synergistic action of oxygen. *Toxicol Sci*. 2003;73(1):60—65.
39. Schlipalius DI, Valmas N, Tuck AG, et al. A core metabolic enzyme mediates resistance to phosphine gas. *Science*. 2012;338(6108):807—810.
40. Link CD. Expression of human beta-amyloid peptide in transgenic *Caenorhabditis elegans*. *Proc Natl Acad Sci U S A*. 1995;92(20):9368—9372.
41. McColl G, Roberts BR, Gunn AP, et al. The *Caenorhabditis elegans* A beta 1-42 model of Alzheimer disease predominantly expresses A beta 3-42. *J Biol Chem*. 2009;284(34):22697—22702.
42. McColl G, Roberts BR, Pukala TL, et al. Utility of an improved model of amyloid-beta (Abeta(1)(-)(4)(2)) toxicity in *Caenorhabditis elegans* for drug screening for Alzheimer's disease. *Mol Neurodegener*. 2012;7,e57.
43. Wu Y, Wu Z, Butko P, et al. Amyloid-beta-induced pathological behaviors are suppressed by Ginkgo biloba extract EGb 761 and ginkgolides in transgenic *Caenorhabditis elegans*. *J Neurosci*. 2006;26(50):13102—13113.
44. Mathew MD, Mathew ND, Ebert PR. WormScan: a technique for high-throughput phenotypic analysis of *Caenorhabditis elegans*. *PLoS One*. 2012;7(3), e33483.
45. Kamath RS, Ahringer J. Genome-wide RNAi screening in *Caenorhabditis elegans*. *Methods*. 2003;30(4):313—321.
46. Sutphin GL, Kaeberlein M. Measuring *Caenorhabditis elegans* life span on solid media. *J Vis Exp*. 2009;27,e1152.
47. Mahoney TR, Luo S, Nonet ML. Analysis of synaptic transmission in *Caenorhabditis elegans* using an aldicarb-sensitivity assay. *Nat Protoc*. 2006;1(4):1772—1777.
48. Lewis JA, Elmer JS, Skimming J, McLafferty S, Fleming J, McGee T. Cholinergic receptor mutants of the nematode *Caenorhabditis elegans*. *J Neurosci*. 1987;7(10):3059—3071.
49. Valmas N, Ebert PR. Comparative toxicity of fumigants and a phosphine synergist using a novel containment chamber for the safe generation of concentrated phosphine gas. *PLoS One*. 2006;1(1),e130.
50. Bargmann CI, Hartwieg E, Horvitz HR. Odorant-selective genes and neurons mediate olfaction in *C. elegans*. *Cell*. 1993;74(3):515—527.
51. Zuryn S, Kuang J, Tuck A, Ebert PR. Mitochondrial dysfunction in *Caenorhabditis elegans* causes metabolic restructuring, but this is not linked to longevity. *Mech Ageing Dev*. 2010;131(9):554—561.
52. Lee SJ, Hwang AB, Kenyon C. Inhibition of respiration extends *C. elegans* life span via reactive oxygen species that increase HIF-1 activity. *Curr Biol*. 2010;20(23):2131—2136.
53. Sunil K, Narayana B. Spectrophotometric determination of hydrogen peroxide in water and cream samples. *Bull Environ Contam Toxicol*. 2008;81(4):422—426.
54. Sobczyk GJ, Wang J, Weijer CJ. SILAC-based proteomic quantification of chemoattractant-induced cytoskeleton dynamics on a second to minute timescale. *Nat Commun*. 2014;5,e3319.
55. Baumann K, Casewell NR, Ali SA, et al. A ray of venom: combined proteomic and transcriptomic investigation of fish venom composition using barb tissue from the blue-spotted stingray (Neotrygon kuhlii). *J Proteomics*. 2014;109:188—198.
56. Ishihama Y, Oda Y, Tabata T, et al. Exponentially modified protein abundance index (emPAI) for estimation of absolute protein amount in proteomics by the number of sequenced peptides per protein. *Mol Cell Proteomics*. 2005;4(9):1265—1272.
57. Ting L, Cowley MJ, Hoon SL, Guilhaus M, Raftery MJ, Cavicchioli R. Normalization and statistical analysis of quantitative proteomics data generated by metabolic labeling. *Mol Cell Proteomics*. 2009;8(10):2227—2242.

58. Lombardo S, Maskos U. Role of the nicotinic acetylcholine receptor in Alzheimer's disease pathology and treatment. *Neuropharmacology*. 2015;96(Pt B):255—262.
59. Saharia K, Arya U, Kumar R, et al. Reserpine modulates neurotransmitter release to extend lifespan and alleviate age-dependent Abeta proteotoxicity in *Caenorhabditis elegans*. *Exp Gerontol*. 2012;47(2):188—197.
60. Luo Y, Wu Y, Brown M, Link CD. *Caenorhabditis elegans* model for initial screening and mechanistic evaluation of potential new drugs for aging and Alzheimer's disease. In: Buccafusco JJ, ed. *Methods of Behavior Analysis in Neuroscience*. 2nd ed. 2009. Boca Raton (FL).
61. Waggoner LE, Zhou GT, Schafer RW, Schafer WR. Control of alternative behavioral states by serotonin in *Caenorhabditis elegans*. *Neuron*. 1998;21(1):203—214.
62. Kayed R, Lasagna-Reeves CA. Molecular mechanisms of amyloid oligomers toxicity. *J Alzheimers Dis*. 2013;33(Suppl 1): S67—S78.
63. Raza H, Prabu SK, John A, Avadhani NG. Impaired mitochondrial respiratory functions and oxidative stress in streptozotocin-induced diabetic rats. *Int J Mol Sci*. 2011; 12(5):3133—3147.
64. Pajak B, Kania E, Orzechowski A. Killing me softly: connotations to unfolded protein response and oxidative stress in Alzheimer's disease. *Oxid Med Cell Longev*. 2016; 2016,e1805304.
65. Misonou H, Morishima-Kawashima M, Ihara Y. Oxidative stress induces intracellular accumulation of amyloid beta-protein (Abeta) in human neuroblastoma cells. *Biochemistry*. 2000; 39(23):6951—6959.
66. Tahara EB, Barros MH, Oliveira GA, Netto LE, Kowaltowski AJ. Dihydrolipoyl dehydrogenase as a source of reactive oxygen species inhibited by caloric restriction and involved in Saccharomyces cerevisiae aging. *FASEB J*. 2007;21(1): 274—283.
67. Murphy MP. How mitochondria produce reactive oxygen species. *Biochem J*. 2009;417(1):1—13.
68. Kalyanaraman B, Darley-Usmar V, Davies KJ, et al. Measuring reactive oxygen and nitrogen species with fluorescent probes: challenges and limitations. *Free Radic Biol Med*. 2012;52(1): 1—6.
69. Zuryn S, Kuang J, Ebert P. Mitochondrial modulation of phosphine toxicity and resistance in *Caenorhabditis elegans*. *Toxicol Sci*. 2008;102(1):179—186.
70. Nath NS, Bhattacharya I, Tuck AG, Schlipalius DI, Ebert PR. Mechanisms of phosphine toxicity. *J Toxicol*. 2011; 2011,e494168.
71. Luis PB, Ruiter JP, Aires CC, et al. Valproic acid metabolites inhibit dihydrolipoyl dehydrogenase activity leading to impaired 2-oxoglutarate-driven oxidative phosphorylation. *Biochim Biophys Acta*. 2007;1767(9):1126—1133.
72. Saada A, Aptowitzer I, Link G, Elpeleg ON. ATP synthesis in lipoamide dehydrogenase deficiency. *Biochem Biophys Res Commun*. 2000;269(2):382—386.
73. Patel MS, Korotchkina LG. Regulation of the pyruvate dehydrogenase complex. *Biochem Soc Trans*. 2006;34(Pt 2): 217—222.
74. Akhtar MW, Sanz-Blasco S, Dolatabadi N, et al. Elevated glucose and oligomeric beta-amyloid disrupt synapses via a common pathway of aberrant protein S-nitrosylation. *Nat Commun*. 2016;7,e10242.
75. Giuffrida ML, Caraci F, Pignataro B, et al. Beta-amyloid monomers are neuroprotective. *J Neurosci*. 2009;29(34): 10582—10587.
76. Giuffrida ML, Tomasello MF, Pandini G, et al. Monomeric β-amyloid interacts with type-1 insulin-like growth factor receptors to provide energy supply to neurons. *Front Cell Neurosci*. 2015;9,e297.
77. Diomede L, Di Fede G, Romeo M, et al. Expression of A2V-mutated Abeta in *Caenorhabditis elegans* results in oligomer formation and toxicity. *Neurobiol Dis*. 2014;62(100):521—532.
78. Kim J, Poole DS, Waggoner LE, et al. Genes affecting the activity of nicotinic receptors involved in *Caenorhabditis elegans* egg-laying behavior. *Genetics*. 2001;157(4):1599—1610.
79. Connop BP, Thies RL, Beyreuther K, Ida N, Reiner PB. Novel effects of FCCP [carbonyl cyanide p-(trifluoromethoxy)phenylhydrazone] on amyloid precursor protein processing. *J Neurochem*. 1999;72(4):1457—1465.
80. Froestl B, Steiner B, Müller WE. Enhancement of proteolytic processing of the beta-amyloid precursor protein by hyperforin. *Biochem Pharmacol*. 2003;66(11):2177—2184.
81. Buckler KJ, Vaughan-Jones RD. Effects of mitochondrial uncouplers on intracellular calcium, pH and membrane potential in rat carotid body type I cells. *J Physiol*. 1998;513(Pt 3):819—833.
82. Itkin A, Dupres V, Dufrene YF, Bechinger B, Ruysschaert JM, Raussens V. Calcium ions promote formation of amyloid beta-peptide (1-40) oligomers causally implicated in neuronal toxicity of Alzheimer's disease. *PLoS One*. 2011;6(3),e18250.
83. Persson T, Popescu BO, Cedazo-Minguez A. Oxidative stress in Alzheimer's disease: why did antioxidant therapy fail? *Oxid Med Cell Longev*. 2014;2014,e427318.
84. Itoh K, Nakamura K, Iijima M, Sesaki H. Mitochondrial dynamics in neurodegeneration. *Trends Cell Biol*. 2013;23(2): 64—71.
85. Tretter L, Adam-Vizi V. Generation of reactive oxygen species in the reaction catalyzed by alpha-ketoglutarate dehydrogenase. *J Neurosci Off J Soc Neurosci*. 2004;24(36):7771—7778.
86. Starkov AA, Fiskum G, Chinopoulos C, et al. Mitochondrial alpha-ketoglutarate dehydrogenase complex generates reactive oxygen species. *J Neurosci*. 2004;24(36):7779—7788.
87. Vaubel RA, Rustin P, Isaya G. Mutations in the dimer interface of dihydrolipoamide dehydrogenase promote site-specific oxidative damages in yeast and human cells. *J Biol Chem*. 2011;286(46):40232—40245.
88. Babady NE, Pang YP, Elpeleg O, Isaya G. Cryptic proteolytic activity of dihydrolipoamide dehydrogenase. *Proc Natl Acad Sci U S A*. 2007;104(15):6158—6163.
89. Proia P, Di Liegro CM, Schiera G, Fricano A, Di Liegro I. Lactate as a metabolite and a regulator in the central nervous system. *Int J Mol Sci*. 2016;17(9),e1450.
90. Iannuzzi C, Irace G, Sirangelo I. The effect of glycosaminoglycans (GAGs) on amyloid aggregation and toxicity. *Molecules*. 2015;20(2):2510—2528.
91. Hernandez-Zimbron LF, Luna-Muñoz J, Mena R, et al. Amyloid-beta peptide binds to cytochrome C oxidase subunit 1. *PLoS One*. 2012;7(8), e42344.
92. Yang S, Wu P, Xiao J, Jiang L. Overexpression of COX6B1 protects against I/Rinduced neuronal injury in rat hippocampal neurons. *Mol Med Rep*. 2019;19(6):4852—4862.
93. Billing O, Kao G, Naredi P. Mitochondrial function is required for secretion of DAF-28/insulin in *C. elegans*. *PLoS One*. 2011; 6(1), e14507.
94. Sontag E, Hladik C, Montgomery L, et al. Downregulation of protein phosphatase 2A carboxyl methylation and methyltransferase may contribute to Alzheimer disease pathogenesis. *J Neuropathol Exp Neurol*. 2004;63(10):1080—1091.
95. Sontag JM, Sontag E. Protein phosphatase 2A dysfunction in Alzheimer's disease. *Front Mol Neurosci*. 2014;7,e16.
96. Petrushanko IY, Mitkevich VA, Anashkina AA, et al. Direct interaction of beta-amyloid with Na,K-ATPase as a putative regulator of the enzyme function. *Sci Rep*. 2016;6,e27738.
97. Clausen MV, Hilbers F, Poulsen H. The structure and function of the Na,K-ATPase isoforms in health and disease. *Front Physiol*. 2017;8,e371.

98. Marshall RS, Vierstra RD. Dynamic regulation of the 26S proteasome: from synthesis to degradation. *Front Mol Biosci*. 2019;6,e40.
99. Motosugi R, Murata S. Dynamic regulation of proteasome expression. *Front Mol Biosci*. 2019;6,e30.
100. Van Raamsdonk JM, Hekimi S. Deletion of the mitochondrial superoxide dismutase sod-2 extends lifespan in *Caenorhabditis elegans*. *PLoS Genet*. 2009;5(2), e1000361.
101. Murshid A, Eguchi T, Calderwood SK. Stress proteins in aging and life span. *Int J Hyperthermia*. 2013;29(5):442—447.
102. Yang H, Li X, Zhu L, et al. Heat shock protein inspired nanochaperones restore amyloid-beta homeostasis for preventative therapy of Alzheimer's disease. *Adv Sci (Weinh)*. 2019;6(22),e1901844.
103. Pontarin G, Fijolek A, Pizzo P, et al. Ribonucleotide reduction is a cytosolic process in mammalian cells independently of DNA damage. *Proc Natl Acad Sci U S A*. 2008;105(46):17801—17806.
104. Bozner P, Grishko V, LeDoux SP, Wilson GL, Chyan YC, Pappolla MA. The amyloid beta protein induces oxidative damage of mitochondrial DNA. *J Neuropathol Exp Neurol*. 1997;56(12):1356—1362.